

A Geometric Structure-Preserving Discretization Scheme for Incompressible Linearized Elasticity*

Arzhang Angoshtari[†] Arash Yavari[‡]

6 March 2013

Abstract

In this paper, we present a geometric discretization scheme for incompressible linearized elasticity. We use ideas from discrete exterior calculus (DEC) to write the action for a discretized elastic body modeled by a simplicial complex. After characterizing the configuration manifold of volume-preserving discrete deformations, we use Hamilton's principle on this configuration manifold. The discrete Euler-Lagrange equations are obtained without using Lagrange multipliers. The main difference between our approach and the mixed finite element formulations is that we simultaneously use three different discrete spaces for the displacement field. We explicitly derive the governing equations for the two-dimensional case, where the discrete spaces for the displacement field are constructed by \mathbb{P}_1 polynomials over primal meshes for incompressibility constraint, \mathbb{P}_0 polynomials over dual meshes for the kinetic energy, and \mathbb{P}_1 polynomials over support volumes for the elastic energy, and the discrete space of the pressure field is constructed by \mathbb{P}_0 polynomials over primal meshes. We test the efficiency and robustness of this geometric scheme using some numerical examples. In particular, we do not see any volume locking and/or checkerboarding of pressure in our numerical examples. This suggests that our choice of discrete solution spaces is compatible.

Contents

1	Introduction	2
2	Incompressible Elasticity	4
2.1	Incompressible Finite Elasticity	4
2.2	Incompressible Linearized Elasticity	9
3	Discrete Exterior Calculus	12
3.1	Primal Meshes	13
3.2	Dual Meshes	14
3.3	Discrete Vector Fields	15
3.4	Primal and Dual Discrete Forms	16
3.5	Discrete Operators	16
3.6	Affine Interpolation	19
4	Discrete Configuration Manifold of Incompressible Linearized Elasticity	20
5	Discrete Governing Equations	26
5.1	Kinetic Energy	27
5.2	Elastic Stored Energy	28
5.3	Discrete Euler-Lagrange Equations	31
5.4	Discrete Pressure Field	33

*To appear in the *Computer Methods in Applied Mechanics and Engineering*.

[†]School of Civil and Environmental Engineering, Georgia Institute of Technology, Atlanta, GA 30332.

[‡]School of Civil and Environmental Engineering & The George W. Woodruff School of Mechanical Engineering, Georgia Institute of Technology, Atlanta, GA 30332. E-mail: arash.yavari@ce.gatech.edu.

6 Numerical Examples	35
7 Concluding Remarks	38

1 Introduction

Finding robust numerical schemes for solving incompressible elasticity problems has been of great interest due to important applications of incompressible elasticity, e.g. in analyzing biological systems where soft tissue is usually modeled as an incompressible elastic body (see Whiteley [1] and Yavari [2] and references therein). It is well known that numerical methods that are reliable for compressible elasticity severely fail for the case of incompressible problems (see [3, 4, 5] and references therein). Inaccurate results are usually due to the locking phenomenon. Locking, in general, is the loss of accuracy of the solution of a numerical scheme for the approximation of a parameter-dependent problem as the parameter tends to a critical value [6, 7]. For example, locking appears in plate and shell models as the thickness $d \rightarrow 0$, analysis of incompressible linear elasticity as Poisson's ratio $\nu \rightarrow 1/2$, and heat transfer problems as the ratio of conductivities $\mu \rightarrow 0$. A robust numerical method is uniformly convergent for all values of the parameter of the problem. Babuška and Suri [6] gave precise mathematical definitions for locking and robustness and gave some general results on the characterization of these phenomena.

To this date various numerical schemes have been developed for incompressible elasticity. The finite element (FE) method is one of the best numerical methods for compressible elasticity. However, FE results may be inaccurate in the near-incompressible and incompressible regimes. To overcome this difficulty, many different approaches have been proposed in the literature. The standard FE formulation based on displacements using low-order elements exhibits a poor performance for near-incompressible elasticity. It has been observed that higher order elements can avoid locking in near-incompressible linear elasticity [8]. Another approach is to use discontinuous Galerkin FE methods [9, 10, 11, 12, 1]. In these formulations, independent approximations are used on different elements and the continuity across boundaries of elements is weakly enforced. Nonconforming FE methods can also avoid locking for near-incompressible elasticity [13, 14, 15]. The simplicity of the aforementioned methods is due to the fact that they are based on the displacement variational formulation, and therefore, one does not need to include other variables in the formulation. There are some formulations based on the Hu-Washizu variational principle, where the displacement, strain, and stress are considered as independent variables. The method of enhanced assumed strain introduced by Simo and Rifai [16] and the method of mixed enhanced strain of Kasper and Taylor [17] are both based on the Hu-Washizu variational principle. Another approach that has widely been used for near-incompressible and incompressible elasticity is mixed formulations based on the Hellinger-Reissner variational principle. In the near-incompressible regime, the stress and displacement are both unknowns. For the incompressible regime, the pressure and displacement are the primary unknowns, where the pressure is the Lagrange multiplier of the incompressibility constraint. It was observed that discrete spaces of the displacement and pressure should be compatible [3]. Various mixed formulations have been developed by using different techniques. Brink and Stephan [18] proposed an adaptive coupling of boundary elements and mixed FE method for incompressible elasticity. Cervera et al. [19] developed mixed simplicial elements for incompressible elasticity and plasticity. Discontinuous Galerkin methods have also been used in the mixed formulations, see [20, 21] and references therein. It has been observed that reduced/selective integration techniques that are closely related to mixed formulations are useful for incompressible elasticity [22, 23]. In these methods, the inf-sup stability requirement are also enforced for the displacement and implicit pressure interpolant spaces. Equal-order interpolation with stabilization methods [24] and average nodal pressure elements [25, 26] have also been successfully implemented. Bonet and Burton [25] proposed a linear tetrahedron element that prevents locking by introducing nodal volumes and evaluating nodal pressures in terms of these volumes. Gatica et al. [27] developed a dual-mixed finite element method for incompressible plane elasticity. Hauret et al. [4] introduced a diamond element FE discretization for compressible and incompressible linear and finite elasticity. Using both primal and dual vertices of an arbitrary simplicial mesh for the domain and its barycentric dual mesh, they constructed an associated diamond mesh. They defined interpolation spaces for displacement and pressure supported on the diamond mesh by choosing piecewise linear displacement interpolation on sub-elements and constant pressure interpolation on diamond elements. They proved that the displacement field converges optimally with mesh refinement and also showed that for the problem of linearized incompressible elasticity their scheme satisfies the inf-sup condition, and hence, it is well posed. Alternatively, it is also possible

to use element-free Galerkin methods [28]. Vidal et al. [29] introduced a pseudo-divergence-free element-free Galerkin method using a diffuse divergence for near-incompressible elasticity. Similar techniques have been used by other researchers for developing mesh-free methods for mixed formulations and B-bar methods [30, 31, 32].

The incompressibility constraint can be imposed more directly using the stream function formulation [33]. Because the divergence of the displacement is zero in incompressible linear elasticity, there is a scalar-valued function called stream function whose curl gives the displacement. Then, the weak formulation of incompressible linear elasticity can be rewritten as a fourth-order elliptic problem over scalar functions. Auricchio et al. [33] used an isogeometric interpolation base on Non-Uniform Rational B-Splines (NURBS) [34] to obtain a locking-free isogeometric approach for the stream function formulation. The high continuity across the elements is the key advantage of NURBS functions. The solution of the stream function formulation automatically satisfies the incompressibility constraint, i.e. it is divergence-free by construction.

Another interesting idea in the literature (promoted mainly by Arnold and his coworkers [35]) is to use an “elasticity complex”, which is similar in form to the classical de Rham complex. In fact, Eastwood [36] showed that the linear elasticity complex can be constructed from the de Rham complex. Having a complex for a field theory, one then defines a discrete analogue of the continuum complex. In the case of finite element method, this gives the appropriate finite element spaces for different fields (e.g. displacements and stresses in the case of linear elasticity). This has led to the discovery of several stable mixed finite elements for linear elasticity [35].

Ciarlet and Ciarlet [37] proposed a new approach for finding the solution of planar linear elasticity that may be capable of handling near incompressible case as well. They showed that this problem can be alternatively reformulated as minimization of an associated Lagrangian over the strain field. They defined their finite element space over a triangulation of the reference configuration as the space of 2×2 symmetric matrix fields, which are constant over each triangle of the triangulation, has the same values for the degrees of freedom at common edges of any two distinct triangles, and is curl-curl free. This curl-curl free condition plays the role of the compatibility conditions. Thus, this method enables one to directly obtain the strains and stresses as they are considered the primal unknowns. Another numerical scheme for dealing with incompressibility is the finite volume method. Bijelonja et al. [38] developed a finite volume based method for incompressible linear elasticity using the solution of the integral form of the governing equations and the introduction of pressure as an additional variable. Considering several numerical examples, they concluded that such numerical methods are locking free.

Geometric ideas were first introduced in numerical electromagnetism (see Gross and Kottiuga [39] and references therein). Here the idea is to use some techniques from differential geometry, algebraic topology, and discrete exterior calculus to write the governing equations and constraints in terms of appropriate geometric entities and then look for the solutions in a proper solution space that satisfies the required constraints. The main advantage of such methods is that by construction they are free of traditional numerical artifacts such as loss of energy or momenta. Hirani et al. [40] used discrete exterior calculus to obtain a numerical method for Darcy flow. They used flux and pressure, which are considered to be differential forms, as the primal unknowns and then the numerical method was derived by using the framework provided by discrete exterior calculus for discretizing differential forms and operators that act on forms. Pavlov et al. [41] proposed a structure-preserving discretization scheme for incompressible fluids. Their main idea is that instead of discretizing spatial velocity, one can discretize push-forward of real-valued functions and the Lie derivative operator. They showed that the space of discrete push-forwards is the space of orthogonal, signed doubly-stochastic matrices and the space of discretized Lie derivatives is the space of antisymmetric null-column matrices. They obtained a discrete in space and continuous in time version of Euler equations using the Lagrange-d’Alembert principle for their discrete Lagrangian and then constructed a fully discrete variational integrator by defining a space-discrete/time-discrete Lagrangian.

The problem with elasticity is that unlike electromagnetism that only requires differential forms one needs to consider various types of tensors for elasticity. There have been recent efforts in the literature in geometrizing discrete elasticity. Chao et al. [42] used geometric ideas to introduce an integrator for nonlinear elasticity. Kanso et al. [43] used bundle-valued differential forms for geometrization of stress. Assuming the existence of some discrete scalar-valued and vector-valued discrete differential forms, Yavari [44] presented a discrete theory with ideas for developing a numerical geometric theory. In the present work, we introduce a geometric structure-preserving scheme for linearized incompressible elasticity. First, we show that in the smooth case, the governing equations of incompressible elasticity can be obtained using Hamilton’s principle over the space of divergence-free vector fields without using Lagrange multipliers. Then, we develop a discrete theory for linearized elasticity by assuming the domain to be a simplicial complex and choosing a discrete displacement field, which is a primal

vector field, as our primal unknown. Thus, we do not need to worry about compatibility equations. Then, we use a discrete definition of divergence to specify the space of discrete divergence-free vector fields over a simplicial mesh and choose this space as our solution space. Motivated by the Lagrangian structure of the smooth case, we define a discrete Lagrangian and use Hamilton's principle over the discrete solution space without using Lagrange multipliers. We observe that pressure gradient appears in the discrete governing equations. Finally, we use the discrete Laplace-Beltrami operator to obtain the discrete pressure – a dual 0-form. This can be thought of as a geometric justification for the known fact that using different function spaces for pressure and displacement is crucial for obtaining robust numerical schemes for incompressible elasticity. Finally, we consider some numerical examples that suggest that our method is free of locking and checkerboarding of pressure.

The approach that we use for imposing the incompressibility constraint is equivalent to the method of Lagrange multipliers for obtaining the mixed formulation of incompressible elasticity. We directly use the space of discrete divergence-free displacements given by the DEC theory. This is the deviation of our approach from the FE method: The definition of the discrete divergence implies a specific linear interpolation for displacements. However, we are free to choose other interpolation methods for the displacement field when we calculate the kinetic and elastic energies. Therefore, unlike the FE method, we simultaneously use three different discrete solution spaces for the displacement field, in general. Similar to the mixed FE formulations, discrete solution spaces for the displacement field should be compatible with each other and with the discrete space of the pressure field to obtain a stable numerical scheme. Our numerical examples suggest that a choice of discrete spaces given by \mathbb{P}_1 polynomials over primal meshes for the incompressibility constraint, \mathbb{P}_1 polynomials over support volumes for the elastic energy, and \mathbb{P}_0 polynomials over primal meshes for the pressure field is a compatible choice.

This paper is structured as follows. In §2 we review incompressible linear and nonlinear elasticity, their geometries, and their variational structures. In particular, we derive the governing equations of incompressible finite and linearized elasticity using Hamilton's principle without using Lagrange multipliers by a direct use of the configuration manifold of incompressible elasticity and the Hodge decomposition theorem. Discrete exterior calculus (DEC) specialized to elasticity applications is reviewed in §3. Discrete configuration manifold of 2D incompressible linearized elasticity is studied in detail in §4. In §5, kinetic and elastic energies of a discretized linear elastic body are written in the language of DEC. Using Hamilton's principle in the discrete configuration manifold of discrete incompressible linearized elasticity then gives the discrete Euler-Lagrange equations. Numerical examples in §6 demonstrate the efficiency and lack of any volume locking in our geometric scheme. Conclusions and future directions are discussed in §7.

2 Incompressible Elasticity

In this section, we first review some basic topics in finite and linearized incompressible elasticity. In particular, we study their variational structure and show that the governing equations of incompressible elasticity can be obtained using the variational principle over the space of volume-preserving deformations.

2.1 Incompressible Finite Elasticity

Here, we first review some preliminaries on finite elasticity and then study the variational structure of incompressible finite elasticity, see Marsden and Hughes [45], Yavari, Marsden, and Ortiz [46] for more details. Let an m -dimensional Riemannian manifold $(\mathcal{B}, \mathbf{G})$ with local coordinates $\{X^A\}$ be the material manifold for an elastic body, i.e., in this manifold the body is stress free¹. We assume that ambient space is another Riemannian manifold $(\mathcal{S}, \mathbf{g})$ of dimension $n \geq m$ with local coordinates $\{x^a\}$. Here for the sake of simplicity, we assume that $m = n$. We use $(\cdot, \cdot)_{\mathbf{G}}$ and $(\cdot, \cdot)_{\mathbf{g}}$ to denote the inner product using the metrics \mathbf{G} and \mathbf{g} , respectively. Motion is a diffeomorphism $\varphi : \mathcal{B} \times \mathbb{R} \rightarrow \mathcal{S}$. If we define $\varphi_t := \varphi(\cdot, t) : \mathcal{B} \rightarrow \mathcal{S}$, then we note that $\varphi_t(\mathcal{B}) \subset \mathcal{S}$ is a submanifold of \mathcal{S} and hence it inherits the metric structure of \mathcal{S} . Let $\varphi_X := \varphi(X, \cdot) : \mathbb{R} \rightarrow \mathcal{S}$. Then $\varphi_X(t)$ specifies a curve in \mathcal{S} and so we can define the following vector field covering φ_t :

$$\mathbf{V}(X, t) = \varphi_{X*} \frac{d}{dt} = T_t(\varphi_X) \cdot \frac{d}{dt} = \frac{\partial \varphi(X, t)}{\partial t}, \quad (2.1)$$

¹In general, $(\mathcal{B}, \mathbf{G})$ is the underlying Riemannian manifold of the material manifold, which is where the body is stress-free. See Yavari and Goriely [47, 48, 49] for more details.

where the linear mapping $T_t\varphi_X$ is the derivative of φ_X at point t and $\frac{d}{dt}$ is the unit vector in the tangent space of \mathbb{R} at t . This vector field is called material velocity. If we push forward \mathbf{V} , we obtain the spatial velocity \mathbf{v} , which is a vector field on $\varphi_t(\mathcal{B})$ given by $\mathbf{v}(x, t) = \mathbf{V}(\varphi_t^{-1}(x), t)$. Similarly, one can define the material acceleration \mathbf{A} and the spatial acceleration \mathbf{a} as

$$\mathbf{A}(X, t) = \frac{\partial \mathbf{V}(X, t)}{\partial t}, \quad \mathbf{a}(x, t) = \mathbf{A}(\varphi_t^{-1}(x), t). \quad (2.2)$$

A motion φ is called volume preserving if for every nice set $\mathcal{U} \subset \mathcal{B}$ we have

$$\int_{\varphi_t(\mathcal{U})} dv = \int_{\mathcal{U}} dV, \quad (2.3)$$

where \mathcal{U} is an open set with a piecewise C^1 boundary $\partial\mathcal{U}$ and $dV = \sqrt{\det \mathbf{G}} \, dX^1 \wedge \cdots \wedge dX^n$ and $dv = \sqrt{\det \mathbf{g}} \, dx^1 \wedge \cdots \wedge dx^n$ are the volume forms of \mathcal{B} and \mathcal{S} , respectively. If $\varphi(X, t)$ is a volume-preserving motion then $\operatorname{div} \mathbf{v} = 0$ and its Jacobian $J(X, t) = 1$, where Jacobian is defined as $J = \sqrt{\frac{\det \mathbf{g}}{\det \mathbf{G}}} \det \mathbf{F}$, with $\mathbf{F} = T_X \varphi_t$. Balance of linear momentum reads

$$\rho_0 \mathbf{A} = \rho_0 \mathbf{B} + \operatorname{Div} \mathbf{P}, \quad (2.4)$$

where $\rho_0 = \rho_0(X)$ denotes mass density of \mathcal{B} , \mathbf{B} is the body force, and \mathbf{P} is the first Piola-Kirchhoff stress tensor. The right Cauchy-Green deformation tensor is defined as $\mathbf{C} = \mathbf{F}^T \mathbf{F} = \varphi_t^* \mathbf{g}$. In this work, we consider hyperelastic materials, i.e. we assume existence of a stored energy function $W = W(X, \mathbf{G}, \mathbf{F}, \mathbf{g})$ or $W = W(X, \mathbf{C})$. For such materials we have the following identity

$$\mathbf{P} = \rho_0 \mathbf{g}^\sharp \frac{\partial W}{\partial \mathbf{F}}. \quad (2.5)$$

In the next section, we study the variational structure of incompressible finite elasticity.

2.1.1 Variational Structure of Incompressible Finite Elasticity

Let $\partial_d \mathcal{B}$ denote the subset of $\partial \mathcal{B}$ on which essential boundary conditions are imposed, i.e., $\varphi|_{\partial_d} = \varphi_d$, and let $\partial_\tau \mathcal{B}$ be the portion of $\partial \mathcal{B}$ on which natural boundary conditions $\boldsymbol{\tau} = \langle \mathbf{P}, \mathbf{N}^\flat \rangle$ are imposed, where \mathbf{N} is the outward unit vector field normal to $\partial \mathcal{B}$, $\boldsymbol{\tau}$ is the traction vector, and $\langle \cdot, \cdot \rangle$ denotes the natural pairing of a vector and a form, i.e., contraction of a covariant index of one tensor with a contravariant index of another tensor. We define the space of configurations of \mathcal{B} to be

$$\mathcal{C} = \{ \psi : \mathcal{B} \rightarrow \mathcal{S} \mid \psi = \varphi_d \text{ on } \partial_d \mathcal{B} \}, \quad (2.6)$$

where φ_d denotes the essential boundary condition on $\partial_d \mathcal{B}$. One can show that \mathcal{C} is a C^∞ infinite-dimensional manifold [50]. A tangent vector to a configuration $\psi \in \mathcal{C}$ is the tangent to a curve $c : (-\epsilon, \epsilon) \rightarrow \mathcal{C}$ with $c(0) = \psi$, which is a velocity field \mathbf{U} covering ψ and vanishes on $\partial_d \mathcal{B}$. Therefore, we have

$$T\mathcal{C} = \{ (\psi, \mathbf{U}) \mid \psi \in \mathcal{C}, \mathbf{U} : \mathcal{B} \rightarrow T\psi(\mathcal{B}) \text{ and } \mathbf{U}|_{\partial_d \mathcal{B}} = 0 \}. \quad (2.7)$$

$T\mathcal{C}$ is usually called the space of variations. Let $H^s = W^{s,2}$ be the Sobolev space consisting of all mappings $\xi : \mathcal{B} \rightarrow \mathcal{S}$ such that ξ and all its derivatives up to order s belong to the Hilbert space L^2 . Note that by defining an appropriate inner product on H^s , it is possible to show that H^s is a Hilbert space [3]. The configuration space for incompressible elasticity is

$$\mathcal{C}_{vol} = \{ \psi \in \mathcal{C} \mid J(\psi) = 1 \}. \quad (2.8)$$

Ebin and Marsden [50] showed that if $\mathcal{C} \subset H^s$ then \mathcal{C}_{vol} is a smooth submanifold of \mathcal{C} . The tangent space of \mathcal{C}_{vol} at a configuration $\psi \in \mathcal{C}_{vol}$ is

$$T_\psi \mathcal{C}_{vol} = \{ \mathbf{U} \in T_\psi \mathcal{C} \mid \operatorname{div} (\mathbf{U} \circ \psi^{-1}) = 0 \}. \quad (2.9)$$

²Recall that $\xi : \mathcal{B} \rightarrow \mathbb{R}^n$ belongs to L^2 if it is square integrable, i.e., $\|\xi\|_{L^2}^2 = \int_{\mathcal{B}} \|\xi\|^2 dV < \infty$.

For unconstrained finite elasticity, the Lagrangian $L : TC \rightarrow \mathbb{R}$ is defined as

$$L(\varphi, \mathbf{V}) = K - V, \quad (2.10)$$

where

$$K(\mathbf{V}) = \frac{1}{2} \int_{\mathcal{B}} \rho_0 (\mathbf{V}, \mathbf{V})_g dV = \frac{1}{2} \int_{\mathcal{B}} \rho_0 \|\mathbf{V}\|_g^2 dV, \quad (2.11)$$

$$V(\varphi) = \int_{\mathcal{B}} \rho_0 W(X, \mathbf{F}) dV + \int_{\mathcal{B}} \rho_0 \mathcal{V}_{\mathbf{B}}(\varphi) dV + \int_{\partial_{\tau} \mathcal{B}} \mathcal{V}_{\tau}(\varphi) dA, \quad (2.12)$$

with $D_{\varphi} \mathcal{V}_{\tau} = -\boldsymbol{\tau}$ and $D_{\varphi} \mathcal{V}_{\mathbf{B}} = -\mathbf{B}$, where $\mathbf{B}(X, t) = \mathbf{b}(\varphi(X, t), t)$ is the material body force and D_{φ} denotes derivative with respect to φ . Note that in Euclidian space, one can consider dead loads as $\mathcal{V}_{\tau}(\varphi) = -(\boldsymbol{\tau}, \varphi)_g$ and $\mathcal{V}_{\mathbf{B}}(\varphi) = -(\mathbf{B}, \varphi)_g$. By setting $\delta \int_0^T L dt = 0$ in the time interval $[0, T]$, one obtains the Euler-Lagrange equations for finite elasticity. For unconstrained finite elasticity, the Euler-Lagrange equations are equivalent to the weak form and the strong form of the governing field equations of nonlinear elasticity [45].

For incompressible finite elasticity we require $\delta \int_0^T L dt = 0$ over volume-preserving motions. To solve this problem, one needs to impose the constraint $J = 1$. This can be done by directly imposing the constraint into the Lagrangian using the Lagrange multipliers [51]. An alternative approach, which is more in line with our discretization philosophy, is to consider the Lagrangian (2.10) on TC_{vol} instead of TC as follows [45] (see also [41] for a similar treatment of incompressible perfect fluids). We want to find a curve $\varphi_t \in \mathcal{C}_{vol}$ on the time interval $[0, T]$ with $\varphi_0 = \text{Id}_{\mathcal{B}}$ ($\text{Id}_{\mathcal{B}} : \mathcal{B} \rightarrow \mathcal{B}$ is the identity map) and $\varphi_T = \tilde{\varphi} \in \mathcal{C}_{vol}$ such that

$$I = \delta \int_0^T L(\varphi_t) dt = 0. \quad (2.13)$$

Let $\varphi_{t,s} \in \mathcal{C}_{vol}$ be a variation field such that $\varphi_{t,0} = \varphi_t$ and $\delta\varphi = \frac{d}{ds}|_{s=0} \varphi_{t,s}$ is a vector field in TC_{vol} . We consider proper variations, and therefore, $\varphi_{0,s} = \varphi_0$ and $\varphi_{T,s} = \tilde{\varphi}$. Then, (2.13) is equivalent to

$$I = \left(\frac{d}{ds} \int_0^T L(\varphi_{t,s}, \dot{\varphi}_{t,s}) dt \right) \Big|_{s=0} = 0. \quad (2.14)$$

We have

$$L(\varphi_{t,s}, \dot{\varphi}_{t,s}) = \int_{\mathcal{B}} \left\{ \frac{1}{2} \rho_0 (\dot{\varphi}_{t,s}, \dot{\varphi}_{t,s})_g - \rho_0 W(X, T_X \varphi_{t,s}) - \rho_0 \mathcal{V}_{\mathbf{B}}(\varphi_{t,s}) \right\} dV - \int_{\partial_{\tau} \mathcal{B}} \mathcal{V}_{\tau}(\varphi_{t,s}) dA, \quad (2.15)$$

and, therefore using the metric compatibility and symmetry of the Levi-Civita connection [52], we obtain

$$\begin{aligned} I &= \left(\frac{d}{ds} \int_0^T L(\varphi_{t,s}, \dot{\varphi}_{t,s}) dt \right) \Big|_{s=0} = \int_0^T \left\{ \frac{d}{ds} L(\varphi_{t,s}, \dot{\varphi}_{t,s}) \Big|_{s=0} \right\} dt \\ &= \int_0^T \left\{ \int_{\mathcal{B}} \left[\rho_0 (\dot{\varphi}_t, \nabla_{\frac{\partial}{\partial t}} \delta\varphi)_g - \left\langle \rho_0 \frac{\partial W}{\partial \mathbf{F}}, \nabla(\delta\varphi) \right\rangle + \rho_0 (\mathbf{B}, \delta\varphi)_g \right] dV + \int_{\partial_{\tau} \mathcal{B}} (\boldsymbol{\tau}, \delta\varphi)_g dA \right\} dt, \end{aligned} \quad (2.16)$$

where the components of the two-point tensor $\nabla(\delta\varphi)$ read

$$\left(\nabla(\delta\varphi) \right)^a{}_{|A} = (\delta\varphi)^a{}_{|A} = \frac{\partial(\delta\varphi)^a}{\partial X^A} + (\delta\varphi)^k \gamma_{kl}^a F^l{}_{|A}, \quad (2.17)$$

with γ_{kl}^a denoting the Christoffel symbols of the coordinate system $\{x^a\}$ on \mathcal{S} and

$$\left\langle \rho_0 \frac{\partial W}{\partial \mathbf{F}}, \nabla(\delta\varphi) \right\rangle = \rho_0 \left(\frac{\partial W}{\partial \mathbf{F}} \right)_a{}^A \left(\nabla(\delta\varphi) \right)^a{}_{|A}. \quad (2.18)$$

Because of metric compatibility of the Levi-Civita connection, we have

$$(\dot{\varphi}_t, \nabla_{\frac{\partial}{\partial t}} \delta\varphi)_g = \frac{d}{dt} (\dot{\varphi}_t, \delta\varphi)_g - \left(\nabla_{\frac{\partial}{\partial t}} \dot{\varphi}_t, \delta\varphi \right)_g. \quad (2.19)$$

As we consider proper variations, substitution of (2.19) into (2.16) yields

$$I = - \int_0^T \left\{ \int_{\mathcal{B}} \left[\rho_0 (\mathbf{A} - \mathbf{B}, \delta\varphi)_g + \left\langle \rho_0 \frac{\partial W}{\partial \mathbf{F}}, \nabla(\delta\varphi) \right\rangle \right] dV - \int_{\partial_{\tau} \mathcal{B}} (\boldsymbol{\tau}, \delta\varphi)_g dA \right\} dt. \quad (2.20)$$

The integrand of I is continuous and T is arbitrary, so setting $I = 0$ results in

$$\int_{\mathcal{B}} \left[\rho_0 (\mathbf{A} - \mathbf{B}, \delta\varphi)_g + \left\langle \rho_0 \frac{\partial W}{\partial \mathbf{F}}, \nabla(\delta\varphi) \right\rangle \right] dV - \int_{\partial_{\tau} \mathcal{B}} (\boldsymbol{\tau}, \delta\varphi)_g dA = 0. \quad (2.21)$$

Equation (2.21) is called the weak form of the field equations of incompressible finite elasticity. Now observe that

$$\text{Div} \left\langle \rho_0 \frac{\partial W}{\partial \mathbf{F}}, \delta\varphi \right\rangle = \left\langle \rho_0 \frac{\partial W}{\partial \mathbf{F}}, \nabla(\delta\varphi) \right\rangle + \left\langle \text{Div} \left(\rho_0 \frac{\partial W}{\partial \mathbf{F}} \right), \delta\varphi \right\rangle, \quad (2.22)$$

where $\text{Div} \left\langle \rho_0 \frac{\partial W}{\partial \mathbf{F}}, \delta\varphi \right\rangle = [(\rho_0 \frac{\partial W}{\partial \mathbf{F}})_a^A (\delta\varphi)^a]_{|A}$ and $[\text{Div}(\rho_0 \frac{\partial W}{\partial \mathbf{F}})]_a = (\rho_0 \frac{\partial W}{\partial \mathbf{F}})_a^A |A$. Thus, if \mathbf{N} denotes the unit normal vector field on $\partial\mathcal{B}$, using divergence theorem one concludes that

$$\int_{\partial\mathcal{B}} \left(\left\langle \rho_0 \frac{\partial W}{\partial \mathbf{F}}, \delta\varphi \right\rangle, \mathbf{N} \right)_G dA = \int_{\mathcal{B}} \left\langle \rho_0 \frac{\partial W}{\partial \mathbf{F}}, \nabla(\delta\varphi) \right\rangle dV + \int_{\mathcal{B}} \left\langle \text{Div} \left(\rho_0 \frac{\partial W}{\partial \mathbf{F}} \right), \delta\varphi \right\rangle dV. \quad (2.23)$$

We assume that $\partial\mathcal{B} = \partial_d\mathcal{B} \cup \partial_{\tau}\mathcal{B}$ and $\partial_d\mathcal{B} \cup \partial_{\tau}\mathcal{B} = \emptyset$, and therefore because $\delta\varphi|_{\partial_d} = 0$, we obtain

$$\int_{\partial\mathcal{B}} \left(\left\langle \rho_0 \frac{\partial W}{\partial \mathbf{F}}, \delta\varphi \right\rangle, \mathbf{N} \right)_G dA = \int_{\partial_{\tau}\mathcal{B}} \left(\left\langle \rho_0 \frac{\partial W}{\partial \mathbf{F}}, \delta\varphi \right\rangle, \mathbf{N} \right)_G dA. \quad (2.24)$$

Note that we have

$$\left[\text{Div} \left(\rho_0 \frac{\partial W}{\partial \mathbf{F}} \right) \right]^{\sharp} = \text{Div} \left(\rho_0 \frac{\partial W}{\partial \mathbf{F}} \right)^{\sharp}, \quad (2.25)$$

with $[(\rho_0 \frac{\partial W}{\partial \mathbf{F}})^{\sharp}]^{aA} = g^{ab} (\rho_0 \frac{\partial W}{\partial \mathbf{F}})_b^A$. Substituting (2.23) and (2.24) into (2.21) and using (2.25) yields

$$\int_{\mathcal{B}} \left(\rho_0 \mathbf{A} - \rho_0 \mathbf{B} - \text{Div} \left(\rho_0 \frac{\partial W}{\partial \mathbf{F}} \right)^{\sharp}, \delta\varphi \right)_g dV + \int_{\partial_{\tau}\mathcal{B}} \left(\left\langle \left(\rho_0 \frac{\partial W}{\partial \mathbf{F}} \right)^{\sharp}, \mathbf{N}^{\flat} \right\rangle - \boldsymbol{\tau}, \delta\varphi \right)_g dA = 0. \quad (2.26)$$

Therefore, our problem has been reduced to finding $\varphi_t \in \mathcal{C}_{vol}$ that satisfies (2.26) for every $\delta\varphi \in T\mathcal{C}_{vol}$. Next, we need to use the following lemma.

Lemma 2.1. *Let $\boldsymbol{\xi}$ be a vector field on a Riemannian manifold $(\mathcal{M}, \mathbf{g})$. If for every vector field $\mathbf{w} \in \{\mathbf{z} : \mathcal{M} \rightarrow T\mathcal{M} | \text{div } \mathbf{z} = 0, \mathbf{z}|_{\partial\mathcal{M}} = 0\}$ we have $\int_{\mathcal{M}} (\boldsymbol{\xi}, \mathbf{w})_g dv = 0$, then there exists a function $p : \mathcal{M} \rightarrow \mathbb{R}$ such that $\boldsymbol{\xi} = -\text{div}(p\mathbf{g}^{\sharp})$.*

Proof: Let $\Omega^k(\mathcal{M})$ denote the set of k -forms on \mathcal{M} and assume that \mathcal{M} is a compact oriented Riemannian manifold with smooth boundary $\partial\mathcal{M}$. The inner product of k -forms $\boldsymbol{\alpha}, \boldsymbol{\beta} \in \Omega^k(\mathcal{M})$ is defined as

$$(\boldsymbol{\alpha}, \boldsymbol{\beta})_g = \int_{\mathcal{M}} \boldsymbol{\alpha} \wedge (*\boldsymbol{\beta}) = \int_{\mathcal{M}} \langle \boldsymbol{\alpha}, \boldsymbol{\beta}^{\sharp} \rangle dv, \quad (2.27)$$

where $*$: $\Omega^k(\mathcal{M}) \rightarrow \Omega^{n-k}(\mathcal{M})$ is the Hodge star operator. The Hodge decomposition theorem [50, 53] states that $\Omega^k(\mathcal{M})$ has the following orthogonal decomposition

$$\Omega^k(\mathcal{M}) = \mathbf{d}(\Omega^{k-1}(\mathcal{M})) \oplus \mathfrak{D}_t^k(\mathcal{M}), \quad (2.28)$$

where

$$\mathbf{d}(\Omega^{k-1}(\mathcal{M})) = \{\boldsymbol{\alpha} \in \Omega^k(\mathcal{M}) \mid \exists \boldsymbol{\beta} \in \Omega^{k-1}(\mathcal{M}) \text{ such that } \boldsymbol{\alpha} = \mathbf{d}\boldsymbol{\beta}\}, \quad (2.29)$$

$$\mathfrak{D}_t^k(\mathcal{M}) = \{\boldsymbol{\alpha} \in \Omega_t^k(\mathcal{M}) \mid \boldsymbol{\delta}\boldsymbol{\alpha} = 0\}, \quad (2.30)$$

with $\mathbf{d} : \Omega^k(\mathcal{M}) \rightarrow \Omega^{k+1}(\mathcal{M})$ and $\boldsymbol{\delta} : \Omega^{k+1}(\mathcal{M}) \rightarrow \Omega^k(\mathcal{M})$ denoting the exterior derivative and codifferential operators, respectively, and

$$\Omega_t^k(\mathcal{M}) = \{\boldsymbol{\alpha} \in \Omega^k(\mathcal{M}) \mid \boldsymbol{\alpha} \text{ is tangent to } \partial\mathcal{M}\}. \quad (2.31)$$

Note that the k -form $\boldsymbol{\alpha} \in \Omega^k(\mathcal{M})$ is tangent to $\partial\mathcal{M}$ if the normal part $\boldsymbol{\alpha}_n = i^*(\ast\boldsymbol{\alpha})$ is zero, where $i : \partial\mathcal{M} \hookrightarrow \mathcal{M}$ is the inclusion map [53]³. Thus, if $\boldsymbol{\xi}$ is a vector field on \mathcal{M} , then the one-form $\boldsymbol{\xi}^\flat$ can be written as

$$\boldsymbol{\xi}^\flat = -\mathbf{d}p + \boldsymbol{\gamma}, \quad (2.32)$$

where $p : \mathcal{M} \rightarrow \mathbb{R}$ is a smooth function, $\boldsymbol{\delta}\boldsymbol{\gamma} = 0$, and $\boldsymbol{\gamma}^\sharp$ is parallel to $\partial\mathcal{M}$, i.e., $\boldsymbol{\gamma}^\sharp(q) \in T_q(\partial\mathcal{M})$ for $q \in \partial\mathcal{M}$. Note that $\operatorname{div}(\boldsymbol{\gamma}^\sharp) = -\boldsymbol{\delta}\boldsymbol{\gamma} = 0$, and therefore $\boldsymbol{\gamma}^\sharp$ is a divergence-free vector field parallel to $\partial\mathcal{M}$. Using (2.32), we can write the assumption of the lemma as

$$\int_{\mathcal{M}} (\boldsymbol{\xi}, \mathbf{w})_g dv = \int_{\mathcal{M}} (\boldsymbol{\xi}^\flat, \mathbf{w}^\flat)_g dv = \int_{\mathcal{M}} -(\mathbf{d}p, \mathbf{w}^\flat)_g dv + \int_{\mathcal{M}} (\boldsymbol{\gamma}, \mathbf{w}^\flat)_g dv = 0, \quad (2.33)$$

for an arbitrary divergence-free vector field \mathbf{w} that vanishes on $\partial\mathcal{M}$. Therefore, \mathbf{w} is parallel to $\partial\mathcal{M}$ and because the decomposition (2.28) is orthogonal with respect to the inner product (2.27), $-(\mathbf{d}p, \mathbf{w}^\flat)_g$ is identically zero and hence (2.33) is equivalent to $(\boldsymbol{\gamma}, \mathbf{w}^\flat)_g = 0$, which means that $\boldsymbol{\gamma} = 0$ as $\boldsymbol{\gamma}, \mathbf{w}^\flat \in \mathfrak{D}_t^1(\mathcal{M})$. Thus, we obtain

$$\boldsymbol{\xi}^\flat = -\mathbf{d}p. \quad (2.34)$$

On the other hand, using the identity

$$\frac{\partial g^{ab}}{\partial x^b} = -g^{cb}\gamma_{cb}^a - g^{ac}\gamma_{cb}^b, \quad (2.35)$$

one can write

$$(pg^{ab})_{|b} = g^{ab} \frac{\partial p}{\partial x^b} + p \left(\frac{\partial g^{ab}}{\partial x^b} + g^{cb}\gamma_{cb}^a + g^{ac}\gamma_{cb}^b \right) = g^{ab} \frac{\partial p}{\partial x^b}, \quad (2.36)$$

or equivalently

$$\operatorname{div}(p\mathbf{g}^\sharp) = (\mathbf{d}p)^\sharp. \quad (2.37)$$

Substituting (2.37) into (2.34) yields $\boldsymbol{\xi} = -\operatorname{div}(p\mathbf{g}^\sharp)$. This completes the proof. \blacksquare

Now returning to (2.26), we note that $\delta\varphi$ is arbitrary and, in particular, it can vanish on the boundary. Hence, the first integral on the left hand side of (2.26) should vanish. Now by using Lemma 2.1, we conclude that

$$\rho_0\mathbf{A} - \rho_0\mathbf{B} - \operatorname{Div} \left(\rho_0 \frac{\partial W}{\partial \mathbf{F}} \right)^\sharp = -\operatorname{div}(p\mathbf{g}^\sharp), \quad (2.38)$$

where the time-dependent function $p : \varphi_t(\mathcal{B}) \times \mathbb{R} \rightarrow \mathbb{R}$ is the pressure field. By defining the material pressure field $p_0(X, t) := \varphi_t^\ast p(X) = p(\varphi_t(X), t)$, and noting that the Jacobian of φ_t is unity, we can use the Piola identity [45] to write

$$\operatorname{div}(p\mathbf{g}^\sharp) = \operatorname{Div} \left(p_0 (\mathbf{F}^{-1})^\sharp \right), \quad (2.39)$$

where $(\mathbf{F}^{-1})^\sharp$ is the tensor with components $(\mathbf{F}^{-1})^{aA}$. Substituting (2.39) into (2.38) yields

$$\rho_0\mathbf{A} = \rho_0\mathbf{B} + \operatorname{Div} \left[\left(\rho_0 \frac{\partial W}{\partial \mathbf{F}} \right)^\sharp - p_0 (\mathbf{F}^{-1})^\sharp \right], \quad (2.40)$$

³Note that if \mathbf{X} is a vector field on \mathcal{M} , then \mathbf{X} is tangent to $\partial\mathcal{M}$ if and only if \mathbf{X}^\flat is tangent to $\partial\mathcal{M}$ [53].

which are the governing equations of incompressible finite elasticity. Substituting (2.40) back into (2.26) and using the divergence theorem results in the natural boundary condition

$$\boldsymbol{\tau}|_{\partial\tau\mathcal{B}} = \left\langle \left(\rho_0 \frac{\partial W}{\partial \mathbf{F}} \right)^\sharp - p_0 (\mathbf{F}^{-1})^\sharp, \mathbf{N}^b \right\rangle. \quad (2.41)$$

Note that p is similar to pressure for perfect fluids and can be considered as the force of the constraint [45]. Also (2.40) implies that the first Piola-Kirchhoff stress tensor can be written as $\mathbf{P} = \left(\rho_0 \frac{\partial W}{\partial \mathbf{F}} \right)^\sharp - p_0 (\mathbf{F}^{-1})^\sharp$.

2.2 Incompressible Linearized Elasticity

In this section we first review some preliminary concepts in linearized elasticity and then study the variational structure of incompressible linearized elasticity formulated on a Riemannian manifold. Here we do not use Lagrange multipliers to enforce the incompressibility constraint. Instead, we confine the displacement field to the set of divergence-free vector fields; motion of an incompressible elastic body extremizes the action function in this space.

Linear elasticity can be considered as the linearization of finite elasticity with respect to a reference motion [45, 54]. The linearized Jacobian about the configuration $\overset{\circ}{\varphi}$ reads [45]

$$\mathcal{L}_{\overset{\circ}{\varphi}}(\mathbf{U}) = \overset{\circ}{J} + J \left[(\operatorname{div} \mathbf{u}) \circ \overset{\circ}{\varphi} \right], \quad (2.42)$$

where $\mathbf{u} = \mathbf{U} \circ \overset{\circ}{\varphi}^{-1}$ and $\overset{\circ}{J}$ is the Jacobian of $\overset{\circ}{\varphi}$. For an incompressible motion, we have $J = 1$, and by choosing $\overset{\circ}{\varphi}$ to be the identity map $\operatorname{Id}_{\mathcal{B}}$, we obtain $1 = J(x) \approx J(\operatorname{Id}_{\mathcal{B}}) + J(\operatorname{Id}_{\mathcal{B}}) \operatorname{div} \mathbf{u}$, which yields

$$\operatorname{Div} \mathbf{U} = \operatorname{div} \mathbf{u} = 0. \quad (2.43)$$

Note that (2.43) is the first-order incompressibility condition, i.e., the incompressibility condition is satisfied up to the first order using (2.43). Let $\mathbf{u} = u^a e_a$ be the displacement field. The linearized strain tensor is $\mathbf{e} = \frac{1}{2} \mathfrak{L}_{\mathbf{u}} \mathbf{g}$ with components $e_{ab} = \frac{1}{2}(u_{a|b} + u_{b|a})$. Balance of linear momentum for an isotropic material reads

$$\rho \ddot{\mathbf{u}} = \rho \mathbf{b} + \operatorname{div}(2\mu \mathbf{e}^\sharp + \lambda(\operatorname{tr} \mathbf{e}) \mathbf{g}^\sharp) \quad \text{in } \mathcal{B}, \quad (2.44)$$

or in components

$$\rho \ddot{u}^a = \rho b^a + (2\mu e^{ab} + \lambda u^c{}_{|c} g^{ab})_{|b} \quad \text{in } \mathcal{B}, \quad (2.45)$$

where μ and λ are Lamé constants with

$$\lambda = \frac{E\nu}{(1+\nu)(1-2\nu)}, \quad \mu = \frac{E}{2(1+\nu)}. \quad (2.46)$$

2.2.1 Variational Structure of Incompressible Linearized Elasticity

Let us recall that the stored energy per unit volume, \mathcal{E} of an isotropic linear elastic solid can be written as

$$\mathcal{E} = \mu \langle \mathbf{e}^\sharp, \mathbf{e} \rangle + \frac{\lambda}{2} (\operatorname{tr} \mathbf{e})^2 = \mu e^{ab} e_{ab} + \lambda (e^a{}_a)^2. \quad (2.47)$$

Because of metric compatibility of the Levi-Civita connection, we have $(\nabla \mathbf{u})^b = \nabla \mathbf{u}^b$, or equivalently, $g_{ac}(u^c{}_{|b}) = u_{a|b}$, where ∇ denotes the Levi-Civita connection of g_{ab} . The incompressibility condition reads $\operatorname{div} \mathbf{u} = u^a{}_{|a} = 0$. Therefore, for an incompressible motion we can write

$$e^a{}_a = \frac{1}{2} g^{ab} (u_{a|b} + u_{b|a}) = \frac{1}{2} g^{ab} (g_{ca} u^c{}_{|b} + g_{cb} u^c{}_{|a}) = \frac{1}{2} (\delta^b{}_c u^c{}_{|b} + \delta^a{}_c u^c{}_{|a}) = u^a{}_{|a} = 0. \quad (2.48)$$

Thus, the stored energy per unit volume of an incompressible linear elastic body reads

$$\mathcal{E} = \mu \langle \mathbf{e}^\sharp, \mathbf{e} \rangle = \mu e^{ab} e_{ab}. \quad (2.49)$$

The Cauchy stress tensor of an isotropic linear elastic body can be written as

$$\boldsymbol{\sigma}^b = 2\mu \mathbf{e} + \lambda(\text{tr } \mathbf{e})\mathbf{g}. \quad (2.50)$$

Also we have [45]

$$\text{div } \mathbf{u} = \frac{\text{tr } \boldsymbol{\sigma}}{3k}, \quad (2.51)$$

where $k = (3\lambda + 2\mu)/3$. If $\nu \rightarrow 1/2$, then from (2.46) we see that $k \rightarrow \infty$ and hence $\text{div } \mathbf{u} \rightarrow 0$, i.e., when $\nu = 1/2$ any motion is incompressible. However, the converse is not necessarily true because if $\text{tr } \boldsymbol{\sigma} = 0$ then motion is incompressible for any ν . For example, let x and y be the usual Euclidian coordinate system and consider an elastic planar sheet under uniform tension in the x -direction and uniform compression of the same magnitude in the y -direction. Then, trace of stress vanishes and this sheet undergoes an incompressible (linearized) motion regardless of the value of its Poisson's ratio.

Remark. Note that if $\nu = 1/2$, then the elasticity tensor is neither pointwise stable nor strongly elliptic [45], which leads to coercivity loss in the weak formulation of the problem [3]. This means that the problem is no longer well posed and this is usually called locking. In this case, usually mixed finite element formulations, i.e., approximating displacement and pressure in different finite element spaces, or constrained finite element formulations are used to obtain well-posed weak forms.

The Lagrangian of a linear incompressible isotropic body is written as $L = K - V$, where

$$K = \frac{1}{2} \int_{\mathcal{B}} \rho(\dot{\mathbf{u}}, \dot{\mathbf{u}})_g dv, \quad V = \int_{\mathcal{B}} \mu e^{ab} e_{ab} dv - \int_{\mathcal{B}} \rho(\mathbf{b}, \mathbf{u})_g dv - \int_{\partial\tau\mathcal{B}} (\boldsymbol{\tau}, \mathbf{u})_g da, \quad (2.52)$$

with $\partial\mathcal{B} = \partial_d\mathcal{B} \cup \partial_\tau\mathcal{B}$, where $\partial_d\mathcal{B}$ and $\partial_\tau\mathcal{B}$ denote the portions of the boundary on which displacements and traction are specified, respectively. Let \mathcal{B} and $\partial\mathcal{B}$ be compact orientable Riemannian manifolds (we assume that the orientation of $\partial\mathcal{B}$ is induced from that of \mathcal{B}) and consider the following sets of diffeomorphisms

$$\begin{aligned} \mathcal{D} &= \{\psi : \mathcal{B} \rightarrow \mathcal{B} \mid \psi \text{ is diffeomorphism}\}, \\ \mathcal{D}_{vol} &= \{\psi \in \mathcal{D} \mid \psi \text{ is volume preserving}\}, \\ \mathcal{D}_q &= \{\psi \in \mathcal{D} \mid \psi(q) = q \text{ for all } q \in \partial\mathcal{B}\}, \\ \mathcal{D}_{vol,q} &= \mathcal{D}_{vol} \cap \mathcal{D}_q, \end{aligned} \quad (2.53)$$

and the following sets of vector fields

$$\begin{aligned} \mathfrak{V} &= \{\mathbf{w} : \mathcal{B} \rightarrow T\mathcal{B} \mid \mathbf{w}(q) \in T_q(\partial\mathcal{B}) \text{ for all } q \in \partial\mathcal{B}\}, \\ \bar{\mathfrak{U}} &= \{\mathbf{w} \in \mathfrak{V} \mid \text{div } \mathbf{w} = 0\}, \\ \mathfrak{V}_0 &= \{\mathbf{w} \in \mathfrak{V} \mid \mathbf{w}|_{\partial\mathcal{B}} = 0\}, \\ \mathfrak{U}_0 &= \{\mathbf{w} \in \mathfrak{V} \mid \text{div } \mathbf{w} = 0, \mathbf{w}|_{\partial\mathcal{B}} = 0\}, \\ \mathfrak{U} &= \{\mathbf{w} : \mathcal{B} \rightarrow T\mathcal{B} \mid \text{div } \mathbf{w} = 0, \mathbf{w}|_{\partial_d\mathcal{B}} = 0\}. \end{aligned} \quad (2.54)$$

Then \mathcal{D} , \mathcal{D}_{vol} , \mathcal{D}_q , and $\mathcal{D}_{vol,q}$ are infinite-dimensional Lie groups (under composition) with infinite-dimensional Lie algebras \mathfrak{V} , $\bar{\mathfrak{U}}$, \mathfrak{V}_0 , and \mathfrak{U}_0 , respectively [50]. In fact, \mathcal{D}_{vol} and \mathcal{D}_q are submanifolds (Lie subgroups) of \mathcal{D} and $\mathcal{D}_{vol,q}$ is a submanifold (Lie subgroup) of \mathcal{D}_q . Also, we have $\mathfrak{U}_0 \subset \mathfrak{U}$ and \mathfrak{U} is the tangent space of \mathcal{C}_{vol} defined in (2.8) at the identity map [45], and thus it is an infinite-dimensional manifold and $\mathbf{u}(t)$ is a curve in \mathfrak{U} . For an arbitrary $\mathbf{w} \in \mathfrak{U}$, let $\mathbf{h}_s(t) = \mathbf{u}(t) + s\mathbf{w}(t)$ be the variational field for $\mathbf{u}(t)$ ⁴. The Lagrangian for the

⁴This choice of the variation field is simpler to work with. The general form of the variation field is a one-parameter family of curves $\mathbf{h}_s(t) = \boldsymbol{\psi}(s, t)$, with $\boldsymbol{\psi}(0, t) = \mathbf{u}(t)$ and $\delta\mathbf{u} = d/ds(\boldsymbol{\psi}(s, t))|_{s=0}$, which yields the same result as the above choice.

variation field reads

$$\begin{aligned} L(s) &= \frac{1}{2} \int_{\mathcal{B}} \rho(\dot{\mathbf{u}} + s\dot{\mathbf{w}}, \dot{\mathbf{u}} + s\dot{\mathbf{w}})_g dv - \int_{\mathcal{B}} \mu(\mathbf{e}^\sharp + s\mathbf{e}_w^\sharp, \mathbf{e} + s\mathbf{e}_w) dv \\ &\quad + \int_{\mathcal{B}} \rho(\mathbf{b}, \mathbf{u} + s\mathbf{w})_g dv + \int_{\partial\tau\mathcal{B}} (\boldsymbol{\tau}, \mathbf{u} + s\mathbf{w})_g da, \end{aligned} \quad (2.55)$$

where the components of the tensor $\mathbf{e}_w = \frac{1}{2}\boldsymbol{\xi}_w\mathbf{g}$ are given by

$$(\mathbf{e}_w)_{ab} = \frac{1}{2}(w_{a|b} + w_{b|a}). \quad (2.56)$$

The true motion of a linear incompressible elastic solid satisfies $\delta \int_0^T L dt = 0$ over \mathfrak{U} , i.e.

$$\begin{aligned} \delta \int_0^T L dt &= \frac{d}{ds} \left(\int_0^T L dt \right) \Big|_{s=0} \\ &= \int_0^T \left\{ \int_{\mathcal{B}} [\rho(\dot{\mathbf{u}}, \dot{\mathbf{w}})_g + \rho(\mathbf{b}, \mathbf{w})_g - 2\mu e^{ab}(\mathbf{e}_w)_{ab}] dv + \int_{\partial\tau\mathcal{B}} (\boldsymbol{\tau}, \mathbf{w})_g da \right\} dt \\ &= - \int_0^T \left\{ \int_{\mathcal{B}} [\rho(\ddot{\mathbf{u}} - \mathbf{b}, \mathbf{w})_g + 2\mu e^{ab}(\mathbf{e}_w)_{ab}] dv - \int_{\partial\tau\mathcal{B}} (\boldsymbol{\tau}, \mathbf{w})_g da \right\} dt + (\dot{\mathbf{u}}, \mathbf{w})_g \Big|_0^T = 0. \end{aligned} \quad (2.57)$$

As we consider proper variations, i.e., $\mathbf{w}(0) = \mathbf{w}(T) = 0$, and the integrand of the time integral is continuous, we obtain the following weak form for the linearized incompressible motion

$$\int_{\mathcal{B}} [\rho(\ddot{\mathbf{u}} - \mathbf{b}, \mathbf{w})_g + 2\mu e^{ab}(\mathbf{e}_w)_{ab}] dv - \int_{\partial\tau\mathcal{B}} (\boldsymbol{\tau}, \mathbf{w})_g da = 0. \quad (2.58)$$

Next, we use the following relation that can be verified by direct substitution:

$$\operatorname{div}(2\mu\mathbf{e}^\sharp, \mathbf{w}^\flat) = 2\mu\langle \mathbf{e}^\sharp, \mathbf{e}_w \rangle + \langle \operatorname{div}(2\mu\mathbf{e}^\sharp), \mathbf{w}^\flat \rangle. \quad (2.59)$$

Using (2.59) and the divergence theorem and because $\mathbf{w}|_{\partial_d\mathcal{B}} = 0$, we obtain

$$\int_{\partial\tau\mathcal{B}} (\langle 2\mu\mathbf{e}^\sharp, \mathbf{w}^\flat \rangle, \mathbf{n})_g da = \int_{\partial\mathcal{B}} (\langle 2\mu\mathbf{e}^\sharp, \mathbf{w}^\flat \rangle, \mathbf{n})_g da = \int_{\mathcal{B}} 2\mu\langle \mathbf{e}^\sharp, \mathbf{e}_w \rangle dv + \int_{\mathcal{B}} (\operatorname{div}(2\mu\mathbf{e}^\sharp), \mathbf{w})_g dv, \quad (2.60)$$

where \mathbf{n} is the unit outward normal vector field for $\partial\mathcal{B}$. In components this reads

$$\int_{\partial\tau\mathcal{B}} 2\mu e^{ab} w_b n_a da = \int_{\mathcal{B}} 2\mu e^{ab} (\mathbf{e}_w)_{ab} dv + \int_{\mathcal{B}} (2\mu e^{ab})_{|a} w_b dv. \quad (2.61)$$

Substituting (2.60) into (2.58) yields

$$\int_{\mathcal{B}} (\rho\ddot{\mathbf{u}} - \rho\mathbf{b} - \operatorname{div}(2\mu\mathbf{e}^\sharp), \mathbf{w})_g dv + \int_{\partial\mathcal{B}} (\langle 2\mu\mathbf{e}^\sharp, \mathbf{n}^\flat \rangle - \boldsymbol{\tau}, \mathbf{w})_g da = 0. \quad (2.62)$$

Suppose $\mathbf{w} \in \mathfrak{U}_0 \subset \mathfrak{U}$, then the second term on the left hand side of (2.62) is identically zero and hence by Lemma 2.1, we obtain

$$\rho\ddot{\mathbf{u}} = \rho\mathbf{b} + \operatorname{div}(2\mu\mathbf{e}^\sharp - p\mathbf{g}^\sharp) \quad \text{in } \mathcal{B}, \quad (2.63)$$

where the time-dependent function $p : \mathcal{B} \times \mathbb{R} \rightarrow \mathbb{R}$ is the pressure field. Substituting (2.63) back into (2.62) results in

$$- \int_{\mathcal{B}} (\operatorname{div}(p\mathbf{g}^\sharp), \mathbf{w})_g dv + \int_{\partial\mathcal{B}} (\langle 2\mu\mathbf{e}^\sharp, \mathbf{n}^\flat \rangle - \boldsymbol{\tau}, \mathbf{w})_g da = 0. \quad (2.64)$$

Using the relation

$$\operatorname{div}(p\mathbf{g}^\sharp, \mathbf{w})_g = p \operatorname{div} \mathbf{w} + (\operatorname{div}(p\mathbf{g}^\sharp), \mathbf{w})_g, \quad (2.65)$$

and noting that \mathbf{w} is divergence free, we can use the divergence theorem to write

$$\int_{\mathcal{B}} (\operatorname{div}(p\mathbf{g}^\sharp), \mathbf{w})_g dv = \int_{\mathcal{B}} \operatorname{div}(p\mathbf{g}^\sharp, \mathbf{w})_g dv = \int_{\partial\mathcal{B}} (\langle p\mathbf{g}^\sharp, \mathbf{w}^\flat \rangle, \mathbf{n})_g da = \int_{\partial\mathcal{B}} (\langle p\mathbf{g}^\sharp, \mathbf{n}^\flat \rangle, \mathbf{w})_g da. \quad (2.66)$$

Substitution of (2.66) into (2.64) yields

$$\int_{\partial\mathcal{B}} (\langle 2\mu\mathbf{e}^\sharp - p\mathbf{g}^\sharp, \mathbf{n}^\flat \rangle - \boldsymbol{\tau}, \mathbf{w})_g da = 0. \quad (2.67)$$

Since $\mathbf{w}|_{\partial\mathcal{B}}$ is an arbitrary vector field on $\partial\mathcal{B}$ that vanishes on $\partial_d\mathcal{B}$, (2.67) implies that

$$\boldsymbol{\tau} = \langle 2\mu\mathbf{e}^\sharp - p\mathbf{g}^\sharp, \mathbf{n}^\flat \rangle \quad \text{on } \partial_\tau\mathcal{B}. \quad (2.68)$$

Equations (2.63) and (2.68) are the governing equations and the natural boundary conditions for incompressible linearized elasticity, respectively. In components they read

$$\rho\ddot{u}^a = \rho b^a + (2\mu e^{ab} - p g^{ab})|_b \quad \text{in } \mathcal{B}, \quad (2.69)$$

$$\boldsymbol{\tau}^a = 2\mu e^{ab} n_b - p g^{ab} n_b \quad \text{on } \partial_\tau\mathcal{B}. \quad (2.70)$$

Remark. We observed that the case $\nu = 1/2$ corresponds to an incompressible motion, and therefore it satisfies the governing equations of incompressible elasticity. On the other hand, we know that $\nu = 1/2$ should satisfy equation (2.44) as well. But there is no pressure in the compressible equations and one may wonder how the compressible and incompressible governing equations can be reconciled for this special case. Let $\nu \rightarrow 1/2$. Then, from (2.51) we see that $\operatorname{div} \mathbf{u} \rightarrow 0$, and using (2.50) and (2.48) we conclude that

$$\operatorname{tr} \boldsymbol{\sigma} = 2\mu \operatorname{tr} \mathbf{e} + 3\lambda \operatorname{tr} \mathbf{e} \rightarrow 3\lambda \operatorname{tr} \mathbf{e}. \quad (2.71)$$

Equivalently, by assuming that $\operatorname{tr} \boldsymbol{\sigma}$ is bounded and defining $p = -\operatorname{tr} \boldsymbol{\sigma}/3$, we can write

$$\lambda \operatorname{tr} \mathbf{e} \rightarrow -p. \quad (2.72)$$

Substituting (2.72) into (2.50) and (2.44) results in the balance of linear momentum for incompressible linearized elasticity. Therefore, we have shown that balance of linear momentum for compressible and incompressible linearized elasticity are the same for $\nu = 1/2$.

Remark. The solution space for incompressible fluids is similar to that of incompressible linearized elasticity. Consider the motion of an incompressible fluid in a Riemannian manifold \mathcal{M} . The spatial velocity of the fluid, \mathbf{v} , lies in the set $\mathfrak{F} = \{\mathbf{w} : \mathcal{M} \rightarrow T\mathcal{M} | \operatorname{div} \mathbf{w} = 0 \text{ and } \mathbf{w}(q) \in T_q(\partial\mathcal{M}) \forall q \in \partial\mathcal{M}\}$, which is similar to \mathfrak{U} . The variation of the spatial velocity of an incompressible fluid $\delta\mathbf{v}$ satisfies the so-called Lin constraint [55, 41], i.e., $\delta\mathbf{v} = \dot{\boldsymbol{\xi}} + [\mathbf{v}, \boldsymbol{\xi}]$, where $\boldsymbol{\xi}$ is an arbitrary divergence-free vector field that vanishes at initial and final times, dot denotes derivative with respect to time, and $[\cdot, \cdot]$ is the usual bracket of vector fields (Lie bracket).

3 Discrete Exterior Calculus

The idea of discrete exterior calculus (DEC) is to define discrete versions of the smooth operators of exterior calculus such that some important theorems, e.g. the generalized Stokes' theorem and the naturality with respect to pull-backs remain valid. However, the convergence of these discrete operators to their smooth counterparts and, in particular, the correct topology to investigate such convergence is still vague and needs more work [56]. For an introductory discussion on the connections between DEC and other structure-preserving schemes such as finite element exterior calculus and mimetic methods, see [57] and references therein. In this section we review some topics from DEC. First, we need to review some concepts from algebraic topology and for this we mainly follow Munkres [58].

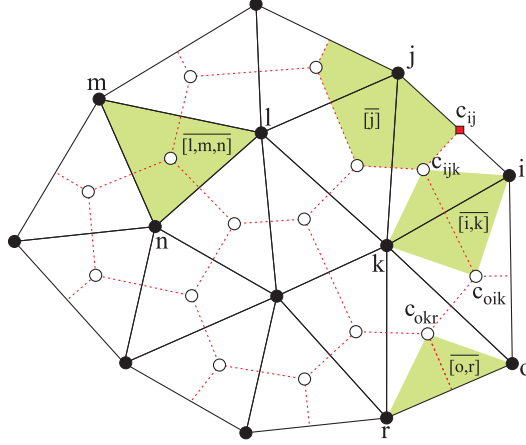


Figure 3.1: A primal 2-dimensional simplicial complex (solid lines) and its dual (dashed lines). The primal vertices are denoted by \bullet and the dual vertices by \circ . The circumcenter $c([i, j, k])$ is denoted by c_{ijk} , etc. The highlighted areas denote the support volumes of the corresponding simplices, for example, $\overline{[i, k]}$ is the support volume of the 1-simplex $[i, k]$. Note that the support volume of the primal vertex j coincides with its dual $\overline{[j]}$ and support volume of the primal 2-simplex $[l, m, n]$ coincides with itself.

3.1 Primal Meshes

Let $\{v_0, \dots, v_k\}$ be a geometrically independent set in \mathbb{R}^N , i.e., $\{v_1 - v_0, \dots, v_k - v_0\}$ is a set of linearly independent vectors in \mathbb{R}^N . The k -simplex σ^k is defined as

$$\sigma^k = \left\{ x \in \mathbb{R}^N \mid x = \sum_{i=0}^k t_i a_i, \text{ where } 0 \leq t_i \leq 1, \sum_{i=0}^k t_i = 1 \right\}. \quad (3.1)$$

The numbers t_i are uniquely determined by x and are called barycentric coordinates of the point x of σ with respect to vertices v_0, \dots, v_k . The number k is the dimension of σ^k . Any simplex σ^l spanned by a subset of vertices $\{v_0, \dots, v_k\}$ is called a face of σ^k and $\sigma^l \prec \sigma^k$ or $\sigma^k \succ \sigma^l$ means that σ^l is a face of σ^k .

A simplicial complex K in \mathbb{R}^N is a collection of simplices in \mathbb{R}^N such that (i) every face of a simplex of K is in K and (ii) the intersection of any two simplices is either empty or a face of each of them. The largest dimension of the simplices of K is called the dimension of K . Fig. 3.1 shows a 2-dimensional simplicial complex with \bullet representing its vertices and the solid lines representing its 1-simplices. A subcomplex of K is a subcollection of K that contains all faces of its elements. The collection of all simplices of K of dimension at most p is called the p -skeleton of K and is denoted by $K^{(p)}$. The subset of \mathbb{R}^N that is the union of the simplices of K is denoted by $|K|$ and is called the underlying space or the polytope of K . The topology on $|K|$ is considered to be the usual subspace topology induced from the ambient space \mathbb{R}^N . A flat simplicial complex K of dimension n in \mathbb{R}^N has all its simplices in the same affine n -space of \mathbb{R}^N , i.e., $|K|$ is a subset of an n -dimensional subset of \mathbb{R}^N that has zero curvature. Here we assume that all simplicial complexes are flat.

A triangulation of a topological space \mathcal{X} is a simplicial complex K with a homeomorphism $\mathfrak{h} : |K| \rightarrow \mathcal{X}$. A differentiable manifold always admits a triangulation [59]. Roughly speaking, triangulation of a differential manifold $\mathcal{M} \subset \mathbb{R}^N$ can be considered as a complex $\mathbb{M} = \mathfrak{h}(K)$ that covers \mathcal{M} and its cells, which in general, have curved faces. A triangulation of the polytope $|K|$ is defined to be any simplicial complex L such that $|L| = |K|$.

Any ordering of the vertices of σ^k defines an orientation for σ^k . We denote the oriented simplex σ^k by $[v_0, \dots, v_k]$. Two orderings of a simplex σ^k are equivalent if one is an even permutation of the other. By definition, a zero simplex has only one orientation. One can see that for $1 \leq k \leq N$, σ^k can have two different orientations. The equivalence class of the particular ordering is denoted by (v_0, \dots, v_k) . Note that the orientation of σ^k induces an orientation on the $(k-1)$ -faces of σ^k defined by $\sigma^{k-1} = (-1)^i [v_0, \dots, \hat{v}_i, \dots, v_k]$, where \hat{v}_i means omit the i th vertex. The ordered collection of vectors $(v_1 - v_0, v_2 - v_0, \dots, v_k - v_0)$ is called a corner basis at v_0 . The span of this basis is called the plane of σ^k and is denoted by $P(\sigma^k)$. The orientation of two oriented simplices σ and τ that have the same dimension can be compared if and only if either they have the same plane or they share a face of dimension $k-1$. If $P(\sigma^k) = P(\tau^k)$, then σ^k and τ^k have the same

orientation if and only if their corner basis orient their plane identically. If σ^k and τ^k have a common $k - 1$ face, then they have the same orientation if and only if the induced orientation by σ^k on the common face is opposite to that induced by τ^k . If two simplices have the same orientations, we write $\text{sgn}(\sigma^k, \tau^k) = +1$, and if they have opposite orientations we write $\text{sgn}(\sigma^k, \tau^k) = -1$. If two simplices have different dimensions, their orientations can not be compared.

A manifold-like simplicial complex K of dimension n is a simplicial complex such that $|K|$ is a topological manifold (possibly with boundary) and each simplex of dimension k with $0 \leq k \leq n - 1$ is a face of an n -simplex in the simplicial complex. A manifold-like simplicial complex of dimension n is called an oriented manifold-like simplicial complex if adjacent n -simplices have the same orientations (orient the common $(n - 1)$ -face oppositely) and simplices of dimensions $n - 1$ and lower are oriented individually. In this work, by the primal mesh we mean a manifold-like oriented simplicial complex.

3.2 Dual Meshes

Dual complexes have an important role in many computational fields. The two most common dual complexes are circumcentric and barycentric dual complexes. The barycentric dual has the nice property that it can be defined for any simplicial complex but the circumcentric dual is well-defined only for well-centered simplicial complexes.⁵ This means that in problems for which one needs to consider a simplicial complex that evolves in time, e.g. finite elasticity, circumcentric dual may not be appropriate. On the other hand, the metric-dependent DEC operators have simpler forms in circumcentric duals [56]. The discretization method that we describe in this paper does not depend on the specific choice of a dual complex as far as a consistent DEC theory is available for that choice of the dual complex. Here we consider circumcentric duals in order to present our method using simpler formulas. Note also that we consider linearized elasticity and hence we are working with a fixed mesh.

The circumcenter of a k -simplex σ^k is the unique point $c(\sigma^k)$ that has the same distance from all the $k + 1$ vertices of σ^k . If $c(\sigma^k)$ lies in the interior of σ^k , then σ^k is called a well-centered simplex. A well-centered simplicial complex is a simplicial complex such that all its simplices (of all dimensions) are well-centered. For example, a planar mesh is well-centered if all of its 2-cells are acute triangles [61]. The (circumcentric) dual complex for an n -dimensional well-centered simplicial complex K is a cell complex $\star K$ with cells $\hat{\sigma}$ defined by the duality operator \star as follows: given a k -simplex σ^k in K , the duality operator gives an $(n - k)$ -cell of $\star K$ as

$$\hat{\sigma}^{n-k} = \star \sigma^k = \sum_{\sigma^k \prec \sigma^{k+1} \prec \dots \prec \sigma^n} \epsilon(\sigma^k, \sigma^{k+1}, \dots, \sigma^n) [c(\sigma^k), c(\sigma^{k+1}), \dots, c(\sigma^n)], \quad (3.2)$$

where the coefficients $\epsilon(\sigma^k, \sigma^{k+1}, \dots, \sigma^n)$ are introduced to glue elements with consistent orientations. Sometimes it is possible to define notions similar to those of a simplicial complex for a dual cell. For example, the dual p -skeleton of K is the union of the cells of dimension at most p of $\star K$ and is denoted by $K_{(p)}$. Fig. 3.1 shows a 2-dimensional simplicial complex (solid lines) together with its dual (dashed lines) where \bullet and \circ denote primal and dual vertices, respectively. Note that dual of a primal vertex is a dual 2-cell, dual of a primal 1-simplex is a dual 1-simplex, and dual of a primal 2-simplex is a dual vertex. For example, denoting $c([i, j, k])$ by c_{ijk} , etc., the dual of the primal 1-simplex $[i, k]$ is either $[c_{ijk}, c_{oik}]$ or $[c_{oik}, c_{ijk}]$ depending on the orientation of the primal mesh.

The support volume $\overline{\sigma^k}$ of a k -simplex σ^k in an n -dimensional complex K is the n -dimensional convex hull of the geometric union of σ^k and $\star \sigma^k$, or equivalently

$$\overline{\sigma^k} = \overline{\star \sigma^k} = \text{convex hull}(\sigma^k, \star \sigma^k) \cap |K|. \quad (3.3)$$

Support volumes of various simplices of a 2-dimensional mesh are shown in Fig. 3.1, where highlighted regions denote the support volumes.

Now we discuss how to orient a dual cell. This is important in the subsequent work. Suppose K is a well-centered n -dimensional primal mesh with the dual $\star K$ and we want to obtain the orientations of the simplices of the dual cell $\hat{\sigma}^k$ that are induced from the orientation of the primal mesh. First we consider the case $1 \leq k \leq n - 1$. Let $\sigma^0, \sigma^1, \dots, \sigma^n$ be primal simplices with $\sigma^0 \prec \sigma^1 \prec \dots \prec \sigma^n$ and let the orientation

⁵Recently, Hirani et al. [60] introduced the notion of signed duals that allows one to work with meshes that are not well-centered as well.

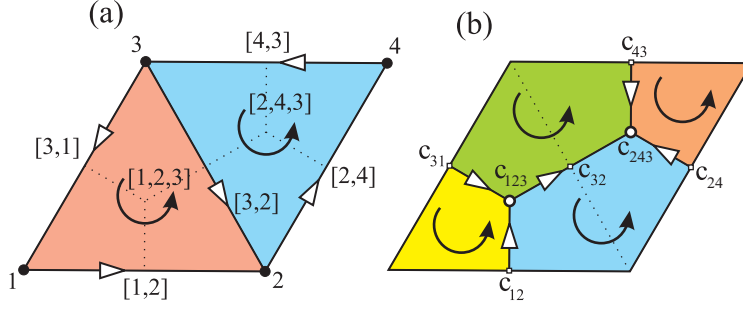


Figure 3.2: *Oriented meshes: (a) primal mesh and (b) associated circumcentric dual mesh. The primal vertices are denoted by \bullet and the dual vertices by \circ . The circumcenter $c([1,2,3])$ is denoted by c_{123} , etc.*

of elementary dual simplices be $s[c(\sigma^k), \dots, c(\sigma^n)]$, where $s = \pm 1$, and the value of s is to be determined. As we mentioned earlier, orientations of σ^k and $[c(\sigma^0), \dots, c(\sigma^k)]$ can be compared as they have the same planes. Similarly, one can compare the orientations of σ^n and $[c(\sigma^0), \dots, c(\sigma^n)]$. Now let us define

$$s = \text{sgn}([c(\sigma^0), \dots, c(\sigma^k)], \sigma^k) \times \text{sgn}([c(\sigma^0), \dots, c(\sigma^n)], \sigma^n). \quad (3.4)$$

If $k = n$, then the dimension of the dual is 0 and hence it can have only one orientation by definition. For $k = 0$ we define $s = \text{sgn}([c(\sigma^0), \dots, c(\sigma^n)], \sigma^n)$. Thus, we note that unlike the primal mesh for which the orientations of the simplices with dimensions less than n are arbitrary, the orientation of none of the simplices of the dual mesh is arbitrary; the dual orientations are induced by the orientation of the primal mesh. The correct orientation of the dual cell is important when we deal with discrete dual forms. In this work by a dual mesh we mean the oriented dual of a well-centered primal mesh. We clarify the previous definitions in the following simple example.

Example 3.1. (Orienting a 2-dimensional Dual Mesh). Consider the 2-dimensional primal mesh and its circumcentric dual shown in Figs. 3.2(a) and (b), respectively. The primal mesh is oriented and we want to obtain the induced orientation of the dual mesh. By definition, orientation of 2-simplices of the dual mesh are the same as those of primal 2-simplices and thus the correct orientation of the dual 2-simplices is counterclockwise. Now consider the dual 1-simplices. As an example, we obtain the orientation of $\star[3,2]$, which consists of two elementary 1-simplices with vertices $\{c_{123}, c_{32}\}$ and $\{c_{243}, c_{32}\}$. The orientation of these elementary simplices is $s_1[c_{32}, c_{123}]$ and $s_2[c_{32}, c_{243}]$, respectively, where

$$\begin{aligned} s_1 &= \text{sgn}([2, c_{32}], [3, 2]) \times \text{sgn}([2, c_{32}, c_{123}], [1, 2, 3]) = (-1) \times (+1) = -1, \\ s_2 &= \text{sgn}([2, c_{32}], [3, 2]) \times \text{sgn}([2, c_{32}, c_{243}], [2, 4, 3]) = (-1) \times (-1) = +1. \end{aligned} \quad (3.5)$$

Thus, the correct orientation of $\star[3,2]$ is $[c_{123}, c_{243}]$. Note that to orient a dual simplex, one needs to orient its elementary duals individually and if the primal mesh is correctly oriented, then these elementary duals will have the same orientations. Similarly, one can obtain the orientations of the other simplices of the dual mesh as is shown in Fig. 3.2(b). Note that there is an easy rule for orienting dual 1-simplices in \mathbb{R}^2 : consider a 1-dimensional face of a primal 2-simplex. If the orientation induced on that face by the orientation of the 2-simplex is the same as the orientation of that face then the direction of the dual of that face points into the 2-simplex, otherwise it points out of the 2-simplex.

3.3 Discrete Vector Fields

As will be explained in the next section, we choose the displacement vector field as our main unknown in incompressible linearized elasticity. Thus, we need to introduce the concept of discrete vector fields on a flat simplicial mesh. Here, there are at least two possibilities: primal and dual vector fields as follows.

A primal discrete vector field \mathbf{X} on an n -dimensional primal mesh K is a map from primal vertices $K^{(0)}$ to \mathbb{R}^n . The space of primal vector fields is denoted by $\mathfrak{X}_d(K)$. One can assume that the value of the primal vector field is constant on each of the n -cells of $\star K$. A dual discrete vector field \mathbf{X} on the dual of an n -dimensional primal mesh K is a map from dual vertices $K_{(0)}$ to \mathbb{R}^n . The space of dual vector fields is denoted by $\mathfrak{X}_d(\star K)$.

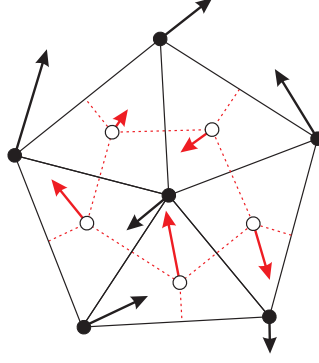


Figure 3.3: A primal vector field (arrows on primal vertices \bullet) and a dual vector field (arrows on dual vertices \circ) on a 2-dimensional mesh. The solid and dashed lines denote the primal and dual meshes, respectively.

One can assume that the value of the dual vector field is constant on each of the n -cells of K . In Fig. 3.3, for a 2-dimensional mesh, primal and dual vectors are denoted by arrows on primal vertices \bullet and dual vertices \circ , respectively.

3.4 Primal and Dual Discrete Forms

In the smooth case, a k -form on an n -manifold \mathcal{N} is an antisymmetric covariant tensor of order k and the set of k -forms on \mathcal{N} is denoted by $\Omega^k(\mathcal{N})$. Now we define primal and dual discrete k -forms. We need the notion of chains and cochains as follows. A k -chain on a simplicial complex K is a function c_k from the set of oriented k -simplices of K to the integers such that (i) $c_k(-\sigma^k) = -c_k(\sigma^k)$, and (ii) $c_k(\sigma) = 0$ for all but finitely many oriented k -simplices σ . If we add k -chains by adding their values, we obtain the group of (oriented) k -chains of K , which is denoted by $C_k(K)$. If $k < 0$ or $k > \dim K$, $C_k(K)$ is defined to be the trivial group. For an oriented simplex σ^k , the elementary chain c corresponding to σ^k is the function defined as

$$c(\tau) = \begin{cases} 1, & \tau = \sigma^k, \\ -1, & \tau = -\sigma^k, \\ 0, & \text{otherwise.} \end{cases} \quad (3.6)$$

In the following the symbol σ^k denotes not only an oriented simplex but also the elementary k -chain c corresponding to σ^k . The meaning is always clear from the context. It can be shown that $C_k(K)$ is free Abelian, i.e., a basis for $C_k(K)$ can be obtained by orienting each k -simplex and using the corresponding elementary chains as a basis. A k -cochain c^k is a homomorphism from the chain group $C_k(K)$ to \mathbb{R} . The space of k -cochains is denoted by $C^k(K) = \text{Hom}(C_k(K), \mathbb{R})$. A primal discrete k -form is a k -cochain and the space of discrete k -forms on K is denoted by $\Omega_d^k(K) = C^k(K)$. Similarly, one can define the space of dual discrete k -forms on $\star K$, which is denoted by $\Omega_d^k(\star K)$. For a k -chain $c_k \in C_k(K)$ and a k -form $\alpha^k \in \Omega_d^k(K)$, we denote the value of α^k at c_k by $\langle \alpha^k, c_k \rangle = \alpha^k(c_k)$. Since $C_k(K)$ is a free Abelian group, we have $c_k = \sum_i \hat{c}_k^i \sigma_i^k$, where $\hat{c}_k^i = c_k(\sigma_i^k) \in \mathbb{Z}$, and summation is over all k -simplices of K . The k -form α^k is a linear function of chains, and thus we have

$$\langle \alpha^k, c_k \rangle = \alpha^k \left(\sum_i \hat{c}_k^i \sigma_i^k \right) = \sum_i \hat{c}_k^i \alpha_i, \quad (3.7)$$

where the coefficients $\alpha_i = \alpha^k(\sigma_i^k) \in \mathbb{R}$ are called the components of the k -form. Thus, one can specify any k -form by a set of real numbers on k -simplices. Similarly, one can define a dual k -form. Fig. 3.4 shows examples of primal and dual 0, 1, and 2-forms on a 2-dimensional mesh.

3.5 Discrete Operators

One of the main goals of this work is to find an appropriate discrete space for displacement field of incompressible linear elasticity, i.e., the discrete space of divergence-free vector fields. Here, we define the discrete divergence

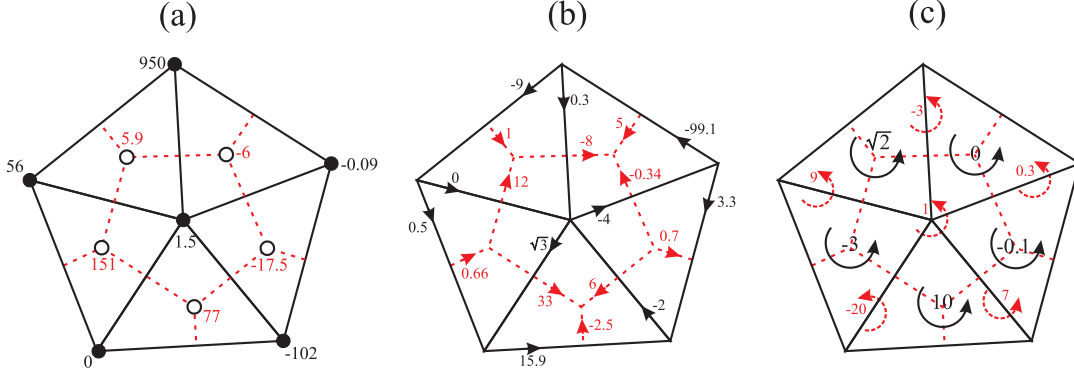


Figure 3.4: Examples of forms on a 2-dimensional primal mesh (solid lines) and its dual mesh (dashed lines): (a) primal and dual 0-forms, which are real numbers on primal and dual vertices, (b) primal and dual 1-forms, which are real numbers on primal and dual 1-simplices, and (c) primal and dual 2-forms, which are real numbers on primal and dual 2-simplices, respectively.

using discrete exterior derivative, discrete Hodge star, and discrete flat operator.

Exterior derivative. The discrete exterior derivative is defined as the coboundary operator as follows. A boundary operator $\partial_k : C_k(K) \rightarrow C_{k-1}(K)$ is a homomorphism defined on each oriented simplex $\sigma^k = [v_0, \dots, v_k]$ as

$$\partial_k \sigma^k = \partial_k [v_0, \dots, v_k] = \sum_{i=0}^k (-1)^i [v_0, \dots, \hat{v}_i, \dots, v_k]. \quad (3.8)$$

The coboundary operator $\delta^k : C^k(K) \rightarrow C^{k+1}(K)$ is defined as

$$\langle \delta^k c^k, c_{k+1} \rangle = \langle c^k, \partial_{k+1} c_{k+1} \rangle. \quad (3.9)$$

Using the above definitions, one can show that $\partial_k \circ \partial_{k+1} = 0$ and $\delta^{k+1} \circ \delta^k = 0$. The sequence

$$0 \rightarrow C_n(K) \xrightarrow{\partial_n} \dots \xrightarrow{\partial_{k+1}} C_k(K) \xrightarrow{\partial_k} \dots \xrightarrow{\partial_1} C_0(K) \rightarrow 0, \quad (3.10)$$

is called the chain complex induced by the boundary operator. Similarly, the sequence

$$0 \leftarrow C^n(K) \xleftarrow{\delta^{n-1}} \dots \xleftarrow{\delta^k} C^k(K) \xleftarrow{\delta^{k-1}} \dots \xleftarrow{\delta^0} C^0(K) \leftarrow 0, \quad (3.11)$$

is called the cochain complex induced by the coboundary operator. The discrete exterior derivative $\mathbf{d} : \Omega_d^k(K) \rightarrow \Omega_d^{k+1}(K)$ is defined to be the coboundary operator δ^k . It follows that $\mathbf{d}^{k+1} \circ \mathbf{d}^k = 0$. Similarly, one can define discrete exterior derivative over a dual mesh. Let K be an n -dimensional primal mesh. Then, the dual boundary operator $\partial_k : C_k(\star K) \rightarrow C_{k-1}(\star K)$ on each oriented dual simplex $\star \sigma^{n-k} = \star [v_0, \dots, v_{n-k}]$ is defined as

$$\partial_k \star [v_0, \dots, v_{n-k}] = \sum_{\sigma^{n-k+1} \succ \sigma^{n-k}} s_{\sigma^{n-k+1}} \star \sigma^{n-k+1}, \quad (3.12)$$

where $s_{\sigma^{n-k+1}} = \pm 1$. If $0 \leq k \leq n-1$, $s_{\sigma^{n-k+1}}$ is chosen such that $s_{\sigma^{n-k+1}} \sigma^{n-k+1}$ induces the same orientation on σ^{n-k} as its original orientation. For $k = n$, s_{σ^1} is chosen such that the orientation of $s_{\sigma^1} \star \sigma^1$ is the same as that induced by $\star \sigma^0$ on its geometric boundary. Note that unlike the primal boundary, the dual boundary of a dual cell is not necessarily the same as its geometric boundary. For example, in Fig. 3.2 the dual boundary of $\star \sigma_2^0$ is $[c_{24}, c_{243}] + [c_{243}, c_{123}] + [c_{123}, c_{12}]$, which is different from the geometric boundary of $\star \sigma_2^0$.

The dual discrete exterior derivative $\mathbf{d} : \Omega_d^k(\star K) \rightarrow \Omega_d^{k+1}(\star K)$ is defined to be the dual coboundary operator defined similar to (3.9) by using dual boundary operator. There is a major difference between the dual discrete exterior derivative and the primal one as we explain next. Consider primal and dual zero-forms on the planar mesh shown in Fig. 3.5. Let $\{f^1, \dots, f^4\}$ and $\{f^{123}, f^{243}\}$ be the values of 0-forms on primal and dual vertices,

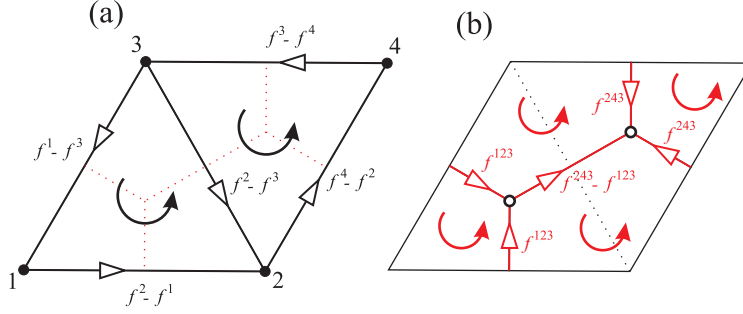


Figure 3.5: The discrete 1-forms $\mathbf{d}f$ obtained from (a) primal and (b) dual 0-form f . The sets $\{f^1, f^2, f^3, f^4\}$ and $\{f^{123}, f^{243}\}$ are the sets of values of primal and dual 0-forms, respectively. Note that f^{123} is the value of f at $c([1, 2, 3])$, etc.

respectively. The value of $\mathbf{d}f$ on the primal and dual 1-simplices are shown in Fig. 3.5(a) and (b), respectively. In the continuous case, we have $\mathbf{d}(f + a) = \mathbf{d}f$, where a is a real constant. The same is true for a primal 0-form as the value of $\mathbf{d}f$ is the differences of values at the end points of each primal 1-simplex. But the value of $\mathbf{d}f$ for dual 1-simplices with one end on the boundary is not the difference of the values at their end points and thus, for a dual 0-form we have $\mathbf{d}(f + a) \neq \mathbf{d}f$. As a consequence, the discrete Laplace-Beltrami operator on dual 0-forms is bijective.

Hodge Star. Recall that in the smooth case, the Hodge star operator $*$: $\Omega^k(\mathcal{N}) \rightarrow \Omega^{n-k}(\mathcal{N})$ for a smooth n -manifold \mathcal{N} , is uniquely defined by the identity [53]

$$\alpha \wedge * \beta = \langle \alpha, \beta^\sharp \rangle \mu, \quad (3.13)$$

where α, β are k -forms and μ is the volume form for \mathcal{N} . For an n -dimensional mesh, the discrete Hodge star is defined as follows. Suppose $1 \leq k \leq n-1$, then the discrete Hodge star operator is a map $*$: $\Omega_d^k(K) \rightarrow \Omega_d^{n-k}(\star K)$ that for a k -simplex σ^k and a discrete k -form α , satisfies the identity

$$\frac{1}{|\star \sigma^k|} \langle * \alpha, \star \sigma^k \rangle = \frac{1}{|\sigma^k|} \langle \alpha, \sigma^k \rangle, \quad (3.14)$$

where $|\sigma^k|$ and $|\star \sigma^k|$ denote the volumes of σ^k and $\star \sigma^k$, respectively. Thus, one can obtain the components of the $(n-k)$ -form $*\alpha$ using the above relation, which uniquely determines $*\alpha$. Note that the left and right-hand sides of (3.14) depend on the orientations of the dual and primal meshes, respectively. But as the primal and dual vertices have only one orientation, by definition, for the cases $k=0$ and $k=n$ one side of (3.14) will be independent of the orientation while the other side changes sign by changing the orientation. Thus, we need to modify the above definition for these cases. For $k=0$ we define

$$\frac{1}{s|\star \sigma^0|} \langle * \alpha, \star \sigma^0 \rangle = \frac{1}{|\sigma^0|} \langle \alpha, \sigma^0 \rangle, \quad (3.15)$$

where we assume the volume of a primal or dual vertex to be +1, i.e., $|\sigma^0| := 1$, and $s = (-1)^{n-1} \text{sgn}(\partial(\star \sigma^0), \star \sigma^1)$, where an edge $\sigma^1 \succ \sigma^0$ pointing away from σ^0 and $\partial(\star \sigma^0)$ has the orientation induced by $\star \sigma^0$. Thus, if the dual of an outgoing 1-simplex has the same orientation as the orientation induced by $\star \sigma^0$, then $s = (-1)^{n-1}$, otherwise $s = (-1)^n$. Similarly, if $k=n$ we define

$$\frac{1}{|\star \sigma^n|} \langle * \alpha, \star \sigma^n \rangle = \frac{1}{s|\sigma^n|} \langle \alpha, \sigma^n \rangle, \quad (3.16)$$

where the value of s is determined as follows. Consider the induced orientation of σ^n on an edge $\sigma^{n-1} \prec \sigma^n$. If $\star \sigma^{n-1}$ points away from $\star \sigma^n$, then $s = (-1)^{n-1}$, otherwise $s = (-1)^n$. Note that the above relations can be used to define the discrete Hodge star as a map $*$: $\Omega_d^k(\star K) \rightarrow \Omega_d^{n-k}(K)$.

Flat Operator. One can define different flat operators, for example, a flat operator that associates a dual 1-form to a primal vector field or a primal 1-form to a dual vector field. Here, we need the former case. Note that Hirani [56] denotes this type of flat operator by b_{pdd} . The discrete flat operator on a primal vector field, $b : \mathfrak{X}_d(K) \rightarrow \Omega_d^1(\star K)$ is defined by its operation on dual elementary chains: given a primal vector field \mathbf{X} and a primal $(n-1)$ -simplex σ^{n-1} , we define

$$\langle \mathbf{X}^b, \star \sigma^{n-1} \rangle = \sum_{\sigma^0 \prec \sigma^{n-1}} \mathbf{X}(\sigma^0) \cdot (\star \sigma^{n-1}), \quad (3.17)$$

where $\star \sigma^{n-1}$ is the vector corresponding to $\star \sigma^{n-1}$, i.e., it has the length $|\star \sigma^{n-1}|$ in the direction of $\star \sigma^{n-1}$, and “ \cdot ” is the usual inner product of \mathbb{R}^n . Using this definition of flat operator, the primal discrete divergence theorem holds automatically. Also note that discrete flat operator is neither surjective nor injective, see Hirani [56] for more discussions.

Divergence. For vector fields on smooth manifolds the following relation holds [53]

$$\operatorname{div} \mathbf{X} = -\delta \mathbf{X}^b = \star \mathbf{d} \star \mathbf{X}^b, \quad (3.18)$$

where $\delta : \Omega^{k+1}(\mathcal{N}) \rightarrow \Omega^k(\mathcal{N})$ is the codifferential operator. Since we have already defined the discrete flat operator, discrete Hodge star, and discrete exterior derivative, we can directly use (3.18) as the definition of the discrete divergence as follows. Let \mathbf{X} be a primal vector field, then the discrete divergence $\operatorname{div} \mathbf{X}$ is the dual 0-form given by

$$\langle \operatorname{div} \mathbf{X}, \star \sigma^n \rangle = \star \mathbf{d} \star \mathbf{X}^b. \quad (3.19)$$

Then, the following divergence theorem holds on a primal mesh, which can be proved by a direct calculation, see Lemma 6.1.6 of [56].

Divergence Theorem on a Primal Mesh. Let K be an n -dimensional primal mesh and σ^0 be one of its primal vertices. Let \mathbf{X} be a primal vector field on the mesh. Then

$$|\sigma^n| \langle \operatorname{div} \mathbf{X}, \star \sigma^n \rangle = \sum_{\sigma^{n-1} \prec \sigma^n} s_{n-1} |\sigma^{n-1}| \left(\sum_{\sigma^0 \prec \sigma^{n-1}} \mathbf{X}(\sigma^0) \right) \cdot \frac{\star \sigma^{n-1}}{|\star \sigma^{n-1}|}, \quad (3.20)$$

where $s_{n-1} = +1$ if the orientation of σ^n is such that the dual edges $\star \sigma^{n-1}$ point outwards and $s_{n-1} = -1$ otherwise.

In the next section, we show that the discrete divergence on a planar simply-connected mesh is surjective and use this discrete divergence to characterize the space of discrete displacement fields of incompressible linearized elasticity.

Laplace-Beltrami. The smooth Laplace-Beltrami operator $\Delta : \Omega^0(\mathcal{N}) \rightarrow \Omega^0(\mathcal{N})$ is defined as $\Delta = \operatorname{div} \circ \operatorname{grad}$. As the gradient of a smooth function $f : \mathcal{N} \rightarrow \mathbb{R}$ is $(\mathbf{d}f)^\sharp$, we can write

$$\Delta f = \star \mathbf{d} \star [(\mathbf{d}f)^\sharp]^b = \star \mathbf{d} \star \mathbf{d}f. \quad (3.21)$$

We already know the definitions of discrete \mathbf{d} and \star , and hence we can use (3.21) to define the primal and dual discrete Laplace-Beltrami operators $\Delta : \Omega_d^0(K) \rightarrow \Omega_d^0(K)$ and $\Delta : \Omega_d^0(\star K) \rightarrow \Omega_d^0(\star K)$, respectively. Obviously, the smooth Δ operator is not injective. The same is true for the primal discrete Δ operator, but as we will show in the sequel, the dual discrete Δ operator is bijective. In §5 we use the dual discrete Δ operator to calculate the discrete pressure field from the pressure gradient.

3.6 Affine Interpolation

To define the elastic energy, we need to interpolate the discrete displacement field over support volumes. For this we use the so-called \mathbb{P}_1 polynomials [3]. Let $\{\mathbf{r}^i \in \mathbb{R}^n\}_{i=1, \dots, n+1}$ be a set a of $n+1$ geometrically-independent

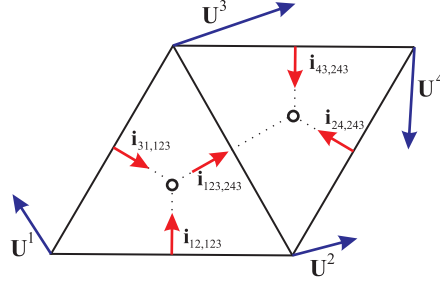


Figure 4.1: A discrete primal vector field, see Fig. 3.2 for the numbering of the simplices and orientation of the primal and dual meshes. The vector $\mathbf{i}_{31,123}$ is the unit vector with the same orientation as $[c_{31}, c_{123}]$, etc.

points that are the vertices of the n -simplex τ^n and suppose that $\{x^i\}$ is the canonical Euclidean coordinate system for \mathbb{R}^n . Let $\{\mathbf{U}^i \in \mathbb{R}^n\}_{i=1, \dots, n+1}$ be a primal vector field on these points, i.e., \mathbf{U}^i is the value of the vector field at the vertex \mathbf{r}^i . For $1 \leq i \leq n+1$, let $\lambda_i: \mathbb{R}^{n+1} \rightarrow \mathbb{R}$ be the associated barycentric coordinates [3]. Then, the interpolating function $\mathfrak{A}: \tau^n \rightarrow \mathbb{R}^n$ is given by $\mathfrak{A}(x^1, \dots, x^n) = \sum_{i=1}^{n+1} \lambda_i(x^1, \dots, x^n) \mathbf{U}^i$, and we have $\mathfrak{A}(\mathbf{r}^i) = \mathbf{U}^i$. Alternatively, it is easier to use the following non-standard form:

$$\mathfrak{A}(x^1, \dots, x^n) = \mathbf{q}^{n+1} + \sum_{i=1}^n x^i \mathbf{q}^i, \quad (3.22)$$

where the constant vectors $\mathbf{q}^i \in \mathbb{R}^n$, $i = 1, \dots, n+1$, are given by

$$\mathbf{q}^i = \sum_{j=1}^{n+1} \mathbb{Q}^{ij} \mathbf{U}^j, \quad i = 1, \dots, n+1, \quad (3.23)$$

and the diagonal matrices $\mathbb{Q}^{ij} \in \mathbb{R}^{n \times n}$, $i, j = 1, \dots, n+1$, depend only on \mathbf{r}^i 's and are independent of \mathbf{U}^i 's.

4 Discrete Configuration Manifold of Incompressible Linearized Elasticity

As we mentioned in §2.2, in linearized elasticity one needs to find the unknown displacement field, which is a vector field on the reference configuration of the elastic body. Thus, we need to consider a fixed well-centered primal mesh for representing the reference configuration, and therefore linearized elasticity is similar to fluid mechanics in the sense that both need a fixed mesh. Note that choosing such well-centered primal meshes is always possible in \mathbb{R}^2 as equilateral triangles fill \mathbb{R}^2 , and hence one can always approximate planar regions with these well-centered simplices. Generating well-centered meshes is not a straightforward task, in general. See VanderZee et al. [61] and references therein for further discussions. However, the approach that we develop here can be extended to arbitrary domains by either generating well-centered meshes for that domain or if it is not possible to generate a well-centered mesh, by using another DEC theory that is appropriate for other types of meshes.

We select the displacement field as our primary unknown, which is a primal discrete vector field. Note that by choosing displacement field as our unknown, we do not need to consider compatibility equations. In order to design a structure-preserving scheme, we require that unknown variables remain in the correct space not only when they converge to the final solution, but also during the process of finding the solution. For incompressible elasticity, this means that we need to search in the space of discrete divergence-free vector fields. The configuration space of incompressible elasticity is similar to that of incompressible fluids. Pavlov et al. [41] developed a structure-preserving method for incompressible perfect fluids. In that scheme, they discretized push-forward of real-valued functions and showed that the space of divergence-free vector fields can be described by some orthogonal matrices. However, in order to define their discrete operators, they had to impose a nonholonomic constraint on the orthogonal matrices, which perhaps makes sense for fluids but is not reasonable for elasticity. Here, we propose a different idea for describing the space of discrete divergence-free

vector fields. For better understanding the idea, we return to the primal mesh shown in Fig. 3.2 and calculate the divergence of a discrete primal vector field, see Fig. 4.1. Let \mathbf{U}^i denote the vector field at vertex i . A straightforward calculation using the definitions of the previous section yields

$$\langle \operatorname{div} \mathbf{U}, \star[1, 2, 3] \rangle = \frac{1}{|[1, 2, 3]|} \sum_{i=1}^4 \mathbf{c}_{1i} \cdot \mathbf{U}^i, \quad \langle \operatorname{div} \mathbf{U}, \star[2, 4, 3] \rangle = \frac{1}{|[2, 4, 3]|} \sum_{i=1}^4 \mathbf{c}_{2i} \cdot \mathbf{U}^i, \quad (4.1)$$

where “ \cdot ” denotes the usual inner product and the vectors $\mathbf{c}_{ij} \in \mathbb{R}^2$ are given by

$$\begin{aligned} \mathbf{c}_{11} &= |[3, 1]| \mathbf{i}_{31,123} + |[1, 2]| \mathbf{i}_{12,123}, & \mathbf{c}_{12} &= |[1, 2]| \mathbf{i}_{12,123} - |[3, 2]| \mathbf{i}_{123,243}, \\ \mathbf{c}_{13} &= |[3, 1]| \mathbf{i}_{31,123} - |[3, 2]| \mathbf{i}_{123,243}, & \mathbf{c}_{14} &= \mathbf{0}, \\ \mathbf{c}_{21} &= \mathbf{0}, & \mathbf{c}_{22} &= |[2, 4]| \mathbf{i}_{24,243} + |[3, 2]| \mathbf{i}_{123,243}, \\ \mathbf{c}_{23} &= |[4, 3]| \mathbf{i}_{43,243} + |[3, 2]| \mathbf{i}_{123,243}, & \mathbf{c}_{24} &= |[2, 4]| \mathbf{i}_{24,243} + |[4, 3]| \mathbf{i}_{43,243}, \end{aligned} \quad (4.2)$$

with $\mathbf{i}_{31,123}$ denoting a unit vector with the same orientation as $[c_{31}, c_{123}]$, etc. (see Fig. 4.1). Now we use (4.1) to impose $\operatorname{div} \mathbf{U} = 0$, which results in

$$\mathbb{I}_{2 \times 8} \mathbf{X}_{8 \times 1} = \mathbf{0}, \quad (4.3)$$

where

$$\mathbb{I}_{2 \times 8} = \begin{bmatrix} \mathbf{c}_{11}^\top & \mathbf{c}_{12}^\top & \mathbf{c}_{13}^\top & \mathbf{c}_{14}^\top \\ \mathbf{c}_{21}^\top & \mathbf{c}_{22}^\top & \mathbf{c}_{23}^\top & \mathbf{c}_{24}^\top \end{bmatrix}, \quad \mathbf{X}_{8 \times 1} = \{\mathbf{U}^1, \dots, \mathbf{U}^4\}^\top. \quad (4.4)$$

Note that the matrix \mathbb{I} only depends on the mesh and does not depend on \mathbf{U} .

Remark. The weak form of the incompressibility constraint reads

$$\int_{\mathcal{B}} q \operatorname{div} \mathbf{U} = 0, \quad \forall q \in L^2(\mathcal{B}). \quad (4.5)$$

Using the notation of [3], consider a Lagrange finite element over the mesh of Fig. 4.1, where the displacement field is approximated by continuous \mathbb{P}_1 polynomials and the pressure field by \mathbb{P}_0 polynomials, i.e. the displacement field is continuous and piecewise-linear while the pressure is piecewise-constant over triangles. For the simplex $[1, 2, 3]$, one can write $|[3, 2]| \mathbf{i}_{123,243} = |[1, 2]| \mathbf{i}_{12,123} + |[3, 1]| \mathbf{i}_{31,123}$. Using this relation and the similar one for $[2, 4, 3]$, it is straightforward to show that (4.3) is the same as the discretization of (4.5) via the Lagrange finite elements.

Now let us consider an n -dimensional primal mesh K_h such that $|K_h| \subset \mathbb{R}^n$ is simply connected⁶ and denote the number of primal and dual vertices with P_h and D_h , where h is the diameter of the primal mesh, i.e., $h = \sup \{\operatorname{diam}(\sigma_i^n) | \sigma_i^n \in K\}$, with $\operatorname{diam}(\sigma_k^n) = \sup \{d(x, y) | x, y \in \sigma_k^n\}$, and $d(x, y)$ denotes the standard distance between x and y . Now we impose the essential boundary conditions. Suppose S_h denotes the number of those primal vertices that are located on the boundary of K_h and their displacements are specified. Note that these known displacements can be nonzero or even time dependent. The unknown primal displacement field \mathbf{U} is denoted by $\{\mathbf{U}^i\}_{i=1, \dots, \bar{P}_h}$, where $\bar{P}_h = P_h - S_h$, and \mathbf{U}^i is the displacement at the vertex i . Imposing the incompressibility constraint using the procedure that resulted in (4.3) yields

$$\mathbb{I}_{D_h \times n \bar{P}_h}^h \mathbf{X}_{n \bar{P}_h \times 1} = \mathbf{u}_{D_h \times 1}^h, \quad (4.6)$$

where \mathbb{I}^h is the reduced incompressibility matrix and depends only on the mesh, \mathbf{u}^h depends on the known values of the displacements and also the mesh, and

$$\mathbf{X}_{n \bar{P}_h \times 1} = \left\{ \mathbf{U}_{n \times 1}^1 \dots \mathbf{U}_{n \times 1}^{\bar{P}_h} \right\}^\top. \quad (4.7)$$

Thus, the displacement field is divergence free if and only if the vector \mathbf{X} satisfies (4.6). Note that if the known

⁶We discuss the effect of simply connectedness in the sequel.

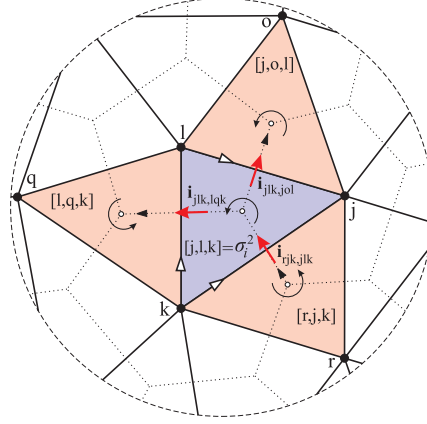


Figure 4.2: A subset of a primal mesh and its associated dual mesh. The vector $\mathbf{i}_{jlk, lqk}$ is the unit vector with the same orientation as $[c([j, l, k]), c([l, q, k])]$, etc.

displacements are all zero, then $\mathbf{u}^h = \mathbf{0}$. There is a systematic way to obtain the reduced incompressibility matrix and \mathbf{u}^h , which is a consequence of the discrete divergence theorem, cf. (3.20). Here we explain the method in \mathbb{R}^2 , but it is also possible to extend it to higher dimensions.

Let $n = 2$ and consider a subset of a 2-dimensional primal mesh and its dual that are shown in Fig. 4.2. We define the matrix $\bar{\mathbb{I}}^h_{D_h \times (2P_h)}$, the incompressibility matrix, as

$$\bar{\mathbb{I}}^h = \begin{bmatrix} \mathbf{c}_{11}^\top & \cdots & \mathbf{c}_{1P_h}^\top \\ \vdots & \ddots & \vdots \\ \mathbf{c}_{D_h 1}^\top & \cdots & \mathbf{c}_{D_h P_h}^\top \end{bmatrix}_{D_h \times (2P_h)}, \quad (4.8)$$

where $\mathbf{c}_{im} \in \mathbb{R}^2$, $i = 1, \dots, D_h$, $m = 1, \dots, P_h$, are specified as follows. Note that the number of the rows of $\bar{\mathbb{I}}^h$ is equal to the number of dual vertices (or equivalently primal 2-cells) as the divergence of a primal vector field is a dual zero-form. Now suppose that we order primal vertices and primal 2-cells of the mesh such that the vertices j , l , and k are the j th, l th, and k th primal vertices of the primal mesh, respectively, and $[j, l, k]$ is the i th 2-cell, i.e., $\sigma_i^2 = [j, l, k]$, as shown in Fig. 4.2. Then, in the i th row of $\bar{\mathbb{I}}^h$, \mathbf{c}_{im} is nonzero if and only if the m th primal vertex is a face of the i th primal 2-cell. This means that the only nonzero elements in the i th row corresponding to $\sigma_i^2 = [j, l, k]$, are \mathbf{c}_{ij} , \mathbf{c}_{il} , and \mathbf{c}_{ik} . The vector \mathbf{c}_{ij} is given by

$$\mathbf{c}_{ij} = s_k |[k, j]| \mathbf{i}_{rjk, jlk} + s_l |[l, j]| \mathbf{i}_{jlk, jol}, \quad (4.9)$$

where $\mathbf{i}_{rjk, jlk}$ denotes the unit vector with the same orientation as $[c([r, j, k]), c([j, l, k])]$, etc., and s_k is +1 if the orientation of $[k, j]$ is the same as the orientation induced by $\sigma_i^2 = [j, l, k]$, otherwise $s_k = -1$. One can determine s_l similarly. Here we have $s_k = +1$ and $s_l = -1$. Similarly, we obtain

$$\mathbf{c}_{il} = -|[l, j]| \mathbf{i}_{jlk, jol} - |[k, l]| \mathbf{i}_{jlk, lqk}, \quad \mathbf{c}_{ik} = -|[k, l]| \mathbf{i}_{jlk, lqk} + |[k, j]| \mathbf{i}_{rjk, jlk}. \quad (4.10)$$

Noting that $\mathbf{i}_{jol, jlk} = -\mathbf{i}_{jlk, jol}$, one can rewrite (4.9) and (4.10) as

$$\begin{aligned} \mathbf{c}_{ij} &= |[k, j]| \mathbf{i}_{rjk, jlk} + |[l, j]| \mathbf{i}_{jol, jlk}, \\ \mathbf{c}_{il} &= |[l, j]| \mathbf{i}_{jol, jlk} + |[k, l]| \mathbf{i}_{lqk, jlk}, \\ \mathbf{c}_{ik} &= |[k, l]| \mathbf{i}_{lqk, jlk} + |[k, j]| \mathbf{i}_{rjk, jlk}, \end{aligned} \quad (4.11)$$

which means that for writing nonzero \mathbf{c}_{im} 's for the i th 2-cell, one simply needs to consider unit normal vectors pointing into that cell and then consider all those terms with a plus sign in each nonzero \mathbf{c}_{im} 's. Thus, we can write the incompressibility matrix without using the orientation of the primal and dual meshes. The condition

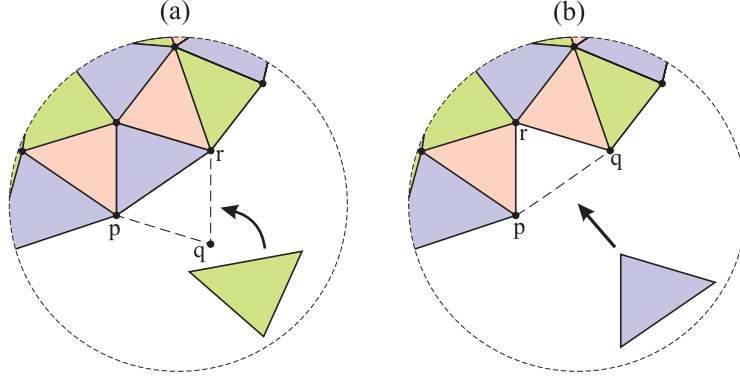


Figure 4.3: Two possible ways for adding a triangle to a 2-dimensional shellable mesh, either (a) the new triangle introduces a new primal vertex or (b) the new triangle does not introduce any new primal vertices.

$\operatorname{div}\mathbf{U} = 0$ is equivalent to

$$\bar{\mathbb{I}}_{D_h \times (2P_h)}^h \bar{\mathbf{X}}_{(2P_h) \times 1} = \mathbf{0}, \quad (4.12)$$

where $\bar{\mathbf{X}}$ is defined similarly to (4.7) but contains both known and unknown displacements.

Suppose $|K_h| \subset \mathbb{R}^2$ is simply connected, i.e., its fundamental group and consequently its first homology group are both trivial. Then, the Euler characteristic of $|K_h|$ reads [62]

$$\chi(|K_h|) = \#(0\text{-simplices}) - \#(1\text{-simplices}) + \#(2\text{-simplices}) = P_h - E_h + D_h = 1, \quad (4.13)$$

where $\#$ denotes “number of” and we have used the fact that the number of 2-simplices of the primal mesh is equal to the number of dual vertices. Let P_h^i and P_h^b denote the number of primal vertices that belong to interior and boundary of $|K_h|$, respectively. Then we have $P_h = P_h^i + P_h^b$. Similarly, let E_h^i and E_h^b denote the number of primal 1-simplices that belong to interior and boundary of $|K_h|$, respectively. We have $E_h = E_h^i + E_h^b$. Using the above definitions, one can show that the following relations hold

$$3D_h = E_h^b + 2E_h^i, \quad P_h^b = E_h^b. \quad (4.14)$$

Using (4.13) and (4.14) we obtain

$$D_h = 2P_h^i + P_h^b - 2 = 2P_h - P_h^b - 2. \quad (4.15)$$

Thus, we always have

$$D_h < 2P_h. \quad (4.16)$$

So, if $\bar{\mathbb{I}}^h$ is full ranked, then $\operatorname{rank}(\bar{\mathbb{I}}^h) = D_h$. Now, we show that the incompressibility matrix of a planar simply-connected mesh is always full ranked.

Theorem 4.1. *Let K_h be a 2-dimensional well-centered primal mesh such that $|K_h|$ is a simply-connected set. Then, the associated incompressibility matrix $\bar{\mathbb{I}}^h$ is full ranked.*

Proof: Since $|K_h|$ is simply connected, because of (4.16) we need to show that the rows of $\bar{\mathbb{I}}^h$ are linearly independent. We use induction to complete the proof. Since K_h is shellable⁷, one can consider a construction of K_h by starting with one triangle and then adding one triangle at a time such that the resulting simplicial complex at each step is homeomorphic to a square. Thus, at each step the mesh has the same topological properties as K_h and, in particular, it is simply connected. Using (4.9) and (4.10), we conclude that the incompressibility matrix of a single triangle is full ranked, i.e., there exist non-zero elements in the matrix since edges of a triangle cannot be parallel to each other. Now suppose that in the process of constructing K_h we have a mesh with m triangles, K^m , that has a full-ranked incompressibility matrix $\bar{\mathbb{I}}_m$, i.e., rows of $\bar{\mathbb{I}}_m$ are linearly independent.

⁷A simplicial complex is called regular if it is homeomorphic to the unit cube. A regular simplicial complex is shellable if either it consists of a single complex or it is possible to obtain a smaller regular complex by removing one of its simplices. All 2-dimensional regular complexes are shellable. Delaunay triangulation of a regular complex is shellable in any dimension [63].

As Fig. 4.3 shows, there are two possibilities for adding a new triangle to K^m : (i) the new triangle adds a new primal vertex to the mesh as in Fig. 4.3(a), and (ii) no new primal vertex is added to the mesh as in Fig. 4.3(b). In case (i) the incompressibility matrix of the resulting mesh, $\bar{\mathbb{I}}_{m+1}$, is full ranked because it is obtained from $\bar{\mathbb{I}}_m$ by adding a row corresponding to the added triangle and two columns for the displacement of the new vertex q (see Fig. 4.3(a)). The only nonzero entries in the new columns are placed on the new row and hence the new row is linearly independent from other rows. In case (ii) note that $\bar{\mathbb{I}}_{m+1}$ is obtained from $\bar{\mathbb{I}}_m$ by adding a new row corresponding to the new primal 2-cell, which has the vertices p , q , and r as is shown in Fig. 4.3(b). The matrix $\bar{\mathbb{I}}_m$ is full ranked and so it has D^m linearly independent columns, where D^m is the number of primal 2-cells of K^m . Thus, because of (4.16), the number of linearly-dependent columns of $\bar{\mathbb{I}}_m$ is equal to $2P^m - D^m = P_m^b + 2$. Due to the structure of $\bar{\mathbb{I}}_m$, one can choose all the independent columns from those that do not correspond to p , q , and r . Suppose that we choose such independent columns. The matrix $\bar{\mathbb{I}}_{m+1}$ is obtained by adding a row to $\bar{\mathbb{I}}_m$ that has zero components except for the ones that correspond to p , q , and r . This means that all the chosen independent columns of $\bar{\mathbb{I}}_m$ still remain independent for $\bar{\mathbb{I}}_{m+1}$ and at least one of the columns that corresponds to p , q , and r becomes independent of other columns. Therefore, $\bar{\mathbb{I}}_{m+1}$ has at least $D^m + 1$ independent columns and since $D^{m+1} = D^m + 1$, we conclude that $\bar{\mathbb{I}}_{m+1}$ has exactly D^{m+1} independent columns and rows, and therefore it is full ranked. This completes the proof. ■

Remark. The assumption of simply connectedness is necessary in the above proof. Note that the incompressibility matrix I is important in our numerical scheme and not \bar{I} . The incompressibility matrix is obtained by removing some rows of \bar{I} and it may or may not remain full-ranked even for a simply-connected domain. Here the important thing is that the number of columns of I remains greater than the number of its rows. This guarantees that the nullity of incompressibility matrix is greater than zero and hence the space of divergence-free vector fields would be a nontrivial finite-dimensional set. For both simply-connected and non-simply-connected domains one can obtain the incompressibility matrix with larger number of columns by mesh refinement.

Also note that the extension of this theorem to 3-dimensional meshes is not straightforward. In particular, a simply-connected mesh in \mathbb{R}^3 is not necessarily shellable. In fact as Rudin [64] shows there exists an unshellable triangulation for a tetrahedron.

Remark. The above theorem tells us that the discrete primal-dual divergence over a planar simply-connected mesh is surjective because the discrete divergence operator from the space of discrete primal vector fields to the space of discrete dual zero-forms is a linear map defined by the matrix $\bar{\mathbb{I}}$. Thus, $\bar{\mathbb{I}}$ being full-ranked implies that the associated linear map is surjective. This is interesting as the discrete flat operator that is used in the definition of divergence is not surjective.

Now let us consider (4.12). In general, using the rank-nullity theorem and (4.16), we can write

$$\text{nullity}(\bar{\mathbb{I}}^h) = 2P_h - \text{rank}(\bar{\mathbb{I}}^h) = 2P_h - D_h = P_h^b + 2 > 0, \quad (4.17)$$

which means that for an arbitrary planar simply-connected mesh, the space of discrete divergence-free primal vector fields is finite-dimensional. In particular if $\{\bar{\mathbf{w}}_i, \dots, \in \mathbb{R}^{2P_h}\}$ is a basis for the null space of $\bar{\mathbb{I}}^h$, we then can write

$$\bar{\mathbf{X}} = \sum_i \hat{D}_i \bar{\mathbf{w}}_i, \quad (4.18)$$

where \hat{D}_i are real numbers. Therefore, a displacement field is divergence free if and only if it can be expressed as in (4.18).

By imposing the essential boundary conditions in (4.12), we obtain (4.6), i.e., \mathbb{I}^h is obtained by eliminating those columns of $\bar{\mathbb{I}}^h$ that correspond to the specified displacements. The vector \mathbf{u}^h is obtained by moving terms that include the specified displacements to the right-hand side of (4.12). If there are “too many” boundary vertices with specified displacements, then the number of rows of \mathbb{I}^h may exceed the number of its columns, and therefore (4.6) may not admit any solution. This is similar to the continuous case where there may not exist a divergence-free vector field for some choices of boundary conditions. We elucidate this in the following example.

Example 4.1. (Incompressibility matrix for a planar mesh). Consider a 2-dimensional mesh consisting of equilateral triangles with unit lengths as shown in Fig. 4.4. Using (4.11), we obtain the incompressibility

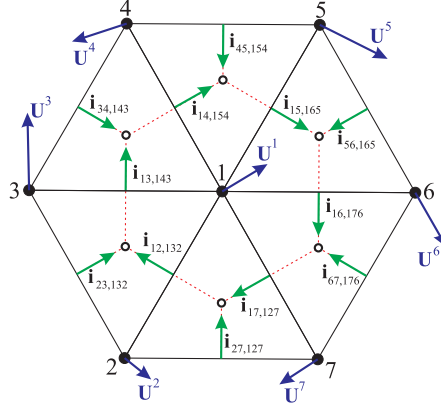


Figure 4.4: A 2-dimensional primal mesh with its associated dual mesh and the associated unit vectors. The vector $\mathbf{i}_{12,132}$ is the unit vector with the same orientation as $[c([1, 2]), c([1, 3, 2])]$, etc.

matrix $\bar{\mathbb{I}}_{6 \times 14}^h$ as

$$\bar{\mathbb{I}}^h = \begin{bmatrix} \mathbf{i}_{12,132} + \mathbf{i}_{143,13} & \mathbf{i}_{12,132} + \mathbf{i}_{23,132} & \mathbf{i}_{23,132} + \mathbf{i}_{143,13} & \mathbf{0} & \mathbf{0} & \mathbf{0} & \mathbf{0} \\ \mathbf{i}_{13,143} + \mathbf{i}_{154,14} & \mathbf{0} & \mathbf{i}_{13,143} + \mathbf{i}_{34,143} & \mathbf{i}_{34,143} + \mathbf{i}_{154,14} & \mathbf{0} & \mathbf{0} & \mathbf{0} \\ \mathbf{i}_{14,154} + \mathbf{i}_{165,15} & \mathbf{0} & \mathbf{0} & \mathbf{i}_{14,154} + \mathbf{i}_{45,154} & \mathbf{i}_{45,154} + \mathbf{i}_{165,15} & \mathbf{0} & \mathbf{0} \\ \mathbf{i}_{15,165} + \mathbf{i}_{176,16} & \mathbf{0} & \mathbf{0} & \mathbf{0} & \mathbf{i}_{15,165} + \mathbf{i}_{56,165} & \mathbf{i}_{56,165} + \mathbf{i}_{176,16} & \mathbf{0} \\ \mathbf{i}_{16,176} + \mathbf{i}_{127,17} & \mathbf{0} & \mathbf{0} & \mathbf{0} & \mathbf{0} & \mathbf{i}_{16,176} + \mathbf{i}_{67,176} & \mathbf{i}_{67,176} + \mathbf{i}_{127,17} \\ \mathbf{i}_{17,127} + \mathbf{i}_{132,12} & \mathbf{i}_{27,127} + \mathbf{i}_{132,12} & \mathbf{0} & \mathbf{0} & \mathbf{0} & \mathbf{0} & \mathbf{i}_{17,127} + \mathbf{i}_{27,127} \end{bmatrix}, \quad (4.19)$$

where \mathbf{i} 's are unit vectors shown in Fig. 4.4 with $\mathbf{i}_{143,13} = -\mathbf{i}_{13,143}$, etc. Also we have

$$\bar{\mathbf{X}}_{14 \times 1} = \{\mathbf{U}^1, \dots, \mathbf{U}^7\}^\top. \quad (4.20)$$

A primal vector field on this mesh is divergence-free if and only if (4.12) is satisfied. Since $\bar{\mathbb{I}}^h$ is full ranked in this example we have $\text{nullity}(\bar{\mathbb{I}}^h) = 14 - 6 = 8$, so we observe that similar to the continuous case where the set of divergence-free vector fields $\tilde{\mathbf{U}}$ defined in (2.54) is nonempty and, in fact, is infinite-dimensional, the set of discrete divergence-free vector fields on this mesh is also nonempty but, of course, it is finite-dimensional. Now suppose that all the boundary vertices have specified displacements, i.e., $\mathbf{U}^i = \tilde{\mathbf{U}}^i$ for $i = 2, \dots, 7$. Then, by moving the terms corresponding to the known displacements to the right-hand side of (4.12), we obtain (4.6), where $\mathbf{X}_{2 \times 1} = \mathbf{U}^1$, with

$$\mathbb{I}_{6 \times 2}^h = \begin{bmatrix} \mathbf{i}_{12,132} + \mathbf{i}_{143,13} \\ \mathbf{i}_{13,143} + \mathbf{i}_{154,14} \\ \mathbf{i}_{14,154} + \mathbf{i}_{165,15} \\ \mathbf{i}_{15,165} + \mathbf{i}_{176,16} \\ \mathbf{i}_{16,176} + \mathbf{i}_{127,17} \\ \mathbf{i}_{17,127} + \mathbf{i}_{132,12} \end{bmatrix}, \quad (4.21)$$

and

$$\mathbf{u}_{6 \times 1}^h = - \left\{ \begin{array}{l} (\mathbf{i}_{12,132} + \mathbf{i}_{23,132}) \cdot \tilde{\mathbf{U}}^2 + (\mathbf{i}_{23,132} + \mathbf{i}_{143,13}) \cdot \tilde{\mathbf{U}}^3 \\ (\mathbf{i}_{13,143} + \mathbf{i}_{34,143}) \cdot \tilde{\mathbf{U}}^3 + (\mathbf{i}_{34,143} + \mathbf{i}_{154,14}) \cdot \tilde{\mathbf{U}}^4 \\ (\mathbf{i}_{14,154} + \mathbf{i}_{45,154}) \cdot \tilde{\mathbf{U}}^4 + (\mathbf{i}_{45,154} + \mathbf{i}_{165,15}) \cdot \tilde{\mathbf{U}}^5 \\ (\mathbf{i}_{15,165} + \mathbf{i}_{56,165}) \cdot \tilde{\mathbf{U}}^5 + (\mathbf{i}_{56,165} + \mathbf{i}_{176,16}) \cdot \tilde{\mathbf{U}}^6 \\ (\mathbf{i}_{16,176} + \mathbf{i}_{67,176}) \cdot \tilde{\mathbf{U}}^6 + (\mathbf{i}_{67,176} + \mathbf{i}_{127,17}) \cdot \tilde{\mathbf{U}}^7 \\ (\mathbf{i}_{27,127} + \mathbf{i}_{132,12}) \cdot \tilde{\mathbf{U}}^2 + (\mathbf{i}_{17,127} + \mathbf{i}_{27,127}) \cdot \tilde{\mathbf{U}}^7 \end{array} \right\}. \quad (4.22)$$

Here it is obvious that (4.6) cannot admit any solutions for some values of the boundary displacements. In our example, if all the boundary displacements vanish, then $\mathbf{X} = \mathbf{0}$ is the only solution. Thus, we see that contrary to the continuous case where the set of divergence-free vector fields that vanish on the boundary of a manifold (\mathfrak{U}_0 defined in (2.54)) is always infinite-dimensional, the corresponding discrete set may only contain the zero vector field.

In general, if

$$2S_h < P_h^b + 2, \quad (4.23)$$

then from (4.15) we have

$$\text{nullity}(\mathbb{I}^h) = 2\bar{P}_h - \text{rank}(\mathbb{I}^h) = 2P_h - 2S_h - \text{rank}(\mathbb{I}^h) \geq 2P_h - D_h - 2S_h = P_h^b + 2 - 2S_h > 0, \quad (4.24)$$

and, therefore, the space of divergence-free vector fields satisfying the essential boundary conditions would be finite-dimensional. Also note that if the essential boundary conditions are not imposed on all the boundary vertices, then one can satisfy (4.23) by choosing finer meshes on that part of the boundary with no essential boundary conditions. To summarize, we observe that the dimension of the space of divergence-free vector fields on a planar simply-connected mesh is $2P_h - D_h$, but by imposing essential boundary conditions, this space may become empty or may contain only the zero vector field.

Let K_h be an n -dimensional primal mesh, possibly not simply-connected and suppose $\text{nullity}(\mathbb{I}^h) = N$. Let $\{\mathbf{w}_i \in \mathbb{R}^{n\bar{P}_h}\}_{i=1}^N$ be a basis for the null space of \mathbb{I}^h . Then, from (4.6) we conclude that if a time-dependent displacement field is divergence-free we have

$$\mathbf{X}(t) = \mathbf{X}^\circ + \sum_{i=1}^N D_i(t) \mathbf{w}_i, \quad (4.25)$$

where \mathbf{X}° is a solution to the inhomogeneous linear system (4.6) and D_i 's are some real-valued functions of time and \mathbf{X}° and \mathbf{w}_i 's are time independent. This completely determines the space of time-dependent displacement fields. Note that if the essential boundary conditions are time dependent, then $\bar{\mathbb{I}}^h$ and so \mathbf{w}_i 's are still time independent but \mathbf{u}^h becomes time dependent, which implies that \mathbf{X}° is time dependent, as well.

Remark. (Non-simply-connected meshes) If K_h has some holes, then (4.12) and (4.14) are still valid but (4.13) reads

$$\chi(|K_h|) = P_h - E_h + D_h = 1 - H, \quad (4.26)$$

where H denotes the number of holes. Thus, (4.15) is replaced by

$$D_h = 2P_h - P_h^b - 2 + 2H, \quad (4.27)$$

and so (4.16) is not necessarily valid. Thus, the effect of holes is similar to the effect of essential boundary conditions in the sense that both can cause the number of the rows of the incompressibility matrix exceed the number of its columns. In particular, note that a non-simply-connected domain may have an incompressibility matrix with the number of its rows exceeding the number of columns even without any essential boundary conditions if there are too many holes in the mesh, i.e., if $P_h^b + 2 < 2H$. Similar to the problems that have too many nodes with essential boundary conditions, here one can obtain an incompressibility matrix with more columns than rows by refining the mesh.

5 Discrete Governing Equations

As we showed in §2.1 and §2.2, incompressible finite and linear elasticity solutions extremize the action in the space of divergence-free motions. This is the procedure that we use for obtaining the governing equations in our discrete formulation. In the previous section, we characterized the space of discrete divergence-free motions in (4.25). Now, we need to write a discrete Lagrangian. We first define discrete kinetic and stored energies in the following.

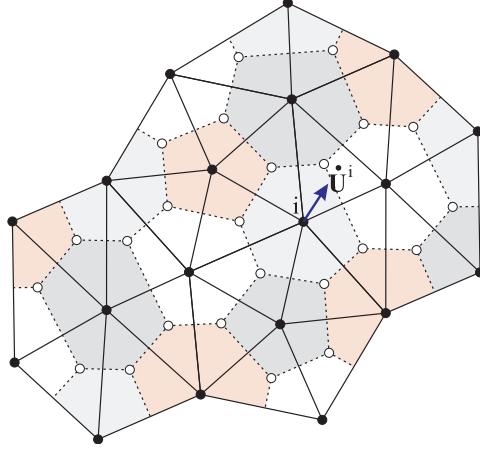


Figure 5.1: Dual cells that are used for defining the kinetic energy. Primal and dual vertices are denoted by \bullet and \circ , respectively. The solid lines denote the boundary of the primal 2-cells and the colored regions denote the dual of each primal vertex. The material properties, displacements, and velocities are considered to be constant on each dual 2-cell. For example, consider the primal vertex i (σ_i^0). The velocity at the corresponding dual cell is assumed to be equal to the velocity at vertex i , which is denoted by $\dot{\mathbf{U}}^i$.

5.1 Kinetic Energy

Let K_h be an n -dimensional mesh. The discrete displacement field is a primal vector field with displacement \mathbf{U}^i at the primal vertex σ_i^0 . As the numbers of primal vertices and dual n -cells are equal, we can associate \mathbf{U}^i to $\star\sigma_i^0$, see Fig. 5.1. This means that we are assuming that the primal mesh is the union of the dual cells and we consider constant displacement and velocity on each dual cell. Suppose we order the primal vertices such that $i = 1, \dots, \bar{P}_h$ denote the primal vertices without essential boundary conditions and $i = \bar{P}_h + 1, \dots, P_h$ denote those primal vertices with essential boundary conditions. We can now define the discrete kinetic energy, K^d , as

$$K^d = \frac{1}{2} \sum_{i=1}^{\bar{P}_h} \rho_i |\star\sigma_i^0| \dot{\mathbf{U}}^i \cdot \dot{\mathbf{U}}^i + \frac{1}{2} \sum_{i=\bar{P}_h+1}^{P_h} \rho_i |\star\sigma_i^0| \dot{\mathbf{U}}^i \cdot \dot{\mathbf{U}}^i, \quad (5.1)$$

where “ \cdot ” denotes the usual dot product and ρ_i is the density on the dual cell $\star\sigma_i^0$, which can have different values on different cells if the elastic body is inhomogeneous. In fact, mass density can be considered as a primal 0-form. Note that time-dependent essential boundary conditions contribute to the kinetic energy through the term

$$K_e^d = \frac{1}{2} \sum_{i=\bar{P}_h+1}^{P_h} \rho_i |\star\sigma_i^0| \dot{\mathbf{U}}^i \cdot \dot{\mathbf{U}}^i, \quad (5.2)$$

but because the variation of K_e^d is zero, it does not contribute to the Euler-Lagrange equations and hence one can safely exclude this term from the following calculations. Using (4.7) we can rewrite the discrete kinetic energy as

$$K^d = \frac{1}{2} \dot{\mathbf{X}}^\top \mathbf{M} \dot{\mathbf{X}} + K_e^d, \quad (5.3)$$

where $\mathbf{M} \in \mathbb{R}^{(n\bar{P}_h) \times (n\bar{P}_h)}$ is a diagonal square matrix with elements

$$M_{jk} = \begin{cases} \rho_i |\star\sigma_i^0|, & \text{if } j = k = n(i-1) + s \quad \text{with } 1 \leq s \leq n, 1 \leq i \leq \bar{P}_h, \\ 0, & \text{if } j \neq k. \end{cases} \quad (5.4)$$

We will use (5.3) to write the discrete Lagrangian.

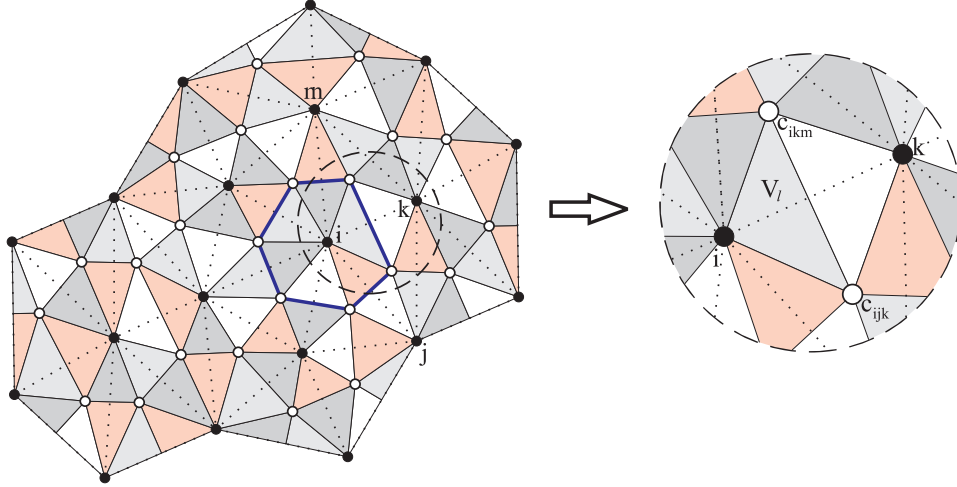


Figure 5.2: Regions that are used for calculating the elastic stored energy. Primal and dual vertices are denoted by \bullet and \circ , respectively. The dotted lines denote the primal one-simplices. Displacement is interpolated using affine functions in each of the colored triangles which are the intersection of a support volume of a primal 1-simplex with a dual 2-cell. The elastic body is assumed to be homogeneous in each dual 2-cell. The region bounded by the solid lines denotes the dual of the primal vertex i . The stored energy at this dual cell is obtained by summing the internal energy of the corresponding 6 smaller triangles.

5.2 Elastic Stored Energy

In this section we define a discrete elastic stored energy. For the sake of clarity, we do not use summation convention throughout this section unless it is explicitly stated otherwise. We order the primal vertices such that $\{\sigma_i^0\}_{i=1}^{\bar{P}_h}$ and $\{\sigma_i^0\}_{i=\bar{P}_h+1}^{\bar{P}_h}$ denote the primal vertices without and with essential boundary conditions, respectively. We define the discrete elastic stored energy as $E^d = \sum_l \mathcal{E}^l$, where \mathcal{E}^l is the internal energy of a portion of support volumes of 1-simplices that is calculated by interpolation of discrete displacements using an affine interpolation function. To fix ideas, we derive the explicit form of the discrete stored energy in \mathbb{R}^2 ($n = 2$). Consider a primal mesh as shown in Fig. 5.2. Discrete stored energy is written as

$$E^d = \sum_l^{2E_h} \mathcal{E}^l, \quad (5.5)$$

where E_h is the number of primal 1-simplices and \mathcal{E}^l 's are the energies associated to the colored regions. This choice of regions follows naturally from our previous assumption of homogeneous material properties within each dual cell and the fact that we need three vertices for a planar affine interpolation. To obtain the explicit form of \mathcal{E}^l , consider the enlarged part of Fig. 5.2 and suppose that i , j , k , and m are the i th, j th, k th, and m th primal vertices, respectively. Here we have $V_l = |\overline{[i, k]} \cap (\star\sigma_i^0)|$, where $\overline{[i, k]}$ denotes the support volume of $[i, k]$ defined in (3.3). Assuming summation convention on indices $a, b = 1, \dots, n$, we define

$$\mathcal{E}^l = \int_{V_l} \mu e^{ab} e_{ab} dv, \quad (5.6)$$

where strains are calculated considering an affine interpolating function for vertices i , c_{ikm} , and c_{ijk} . Using (3.22), let

$$u|_{V_l} = \mathbf{q}_l^{n+1} + \sum_{b=1}^n x^b \mathbf{q}_l^b, \quad (5.7)$$

where $\mathbf{q}_l^b \in \mathbb{R}^n$, $b = 1, \dots, n+1$, are constant vectors associated to V_l that can be written as (see (3.23))

$$\mathbf{q}_l^b = \mathbb{Q}_l^{bi} \mathbf{U}^i + \mathbb{Q}_l^{bc_{ijk}} \mathbf{U}^{c_{ijk}} + \mathbb{Q}_l^{bc_{ikm}} \mathbf{U}^{c_{ikm}}, \quad (5.8)$$

with $\mathbf{U}^{c_{ijk}}$ and $\mathbf{U}^{c_{ikm}}$ denoting displacements of c_{ijk} and c_{ikm} , respectively, and \mathbb{Q}_l^{bi} , $\mathbb{Q}_l^{bc_{ijk}}$, and $\mathbb{Q}_l^{bc_{ikm}}$ defined in §3.6 and are calculated using the vertices i , c_{ijk} , and c_{ikm} . To obtain $\mathbf{U}^{c_{ijk}}$ and $\mathbf{U}^{c_{ikm}}$ we need to interpolate displacements of $\mathfrak{J}_{ijk} = \{i, j, k\}$ and $\mathfrak{J}_{ikm} = \{i, k, m\}$, respectively. Using (3.22) we can write

$$\mathbf{U}^{c_{ijk}} = \sum_{b \in \mathfrak{J}_{ijk}} \mathbb{Q}_{[i,j,k]}^{3b} \mathbf{U}^b + \sum_{a=1}^2 \sum_{b \in \mathfrak{J}_{ijk}} x_{c_{ijk}}^a \mathbb{Q}_{[i,j,k]}^{ab} \mathbf{U}^b, \quad (5.9)$$

$$\mathbf{U}^{c_{ikm}} = \sum_{b \in \mathfrak{J}_{ikm}} \mathbb{Q}_{[i,k,m]}^{3b} \mathbf{U}^b + \sum_{a=1}^2 \sum_{b \in \mathfrak{J}_{ikm}} x_{c_{ikm}}^a \mathbb{Q}_{[i,k,m]}^{ab} \mathbf{U}^b, \quad (5.10)$$

where $x_{c_{ijk}}^a$ and $x_{c_{ikm}}^a$ denote the a -coordinate of c_{ijk} and c_{ikm} , respectively, and the index $[i, j, k]$ in $\mathbb{Q}_{[i,j,k]}^{ab}$ emphasizes that this matrix is obtained by interpolation over $[i, j, k]$. Let $\mathfrak{J}_{ijkm} = \{i, j, k, m\}$, then substituting (5.9) and (5.10) into (5.8) yields

$$\mathbf{q}_l^b = \sum_{a \in \mathfrak{J}_{ijkm}} \mathbb{H}_l^{ba} \mathbf{U}^a, \quad b = 1, 2, 3, \quad (5.11)$$

where by defining $\mathfrak{S} = \{\{i, j, k\}, \{i, k, m\}\}$, we can write $\mathbb{H}_l^{ba} \in \mathbb{R}^{2 \times 2}$ as

$$\begin{aligned} \mathbb{H}_l^{bi} &= \mathbb{Q}_l^{bi} + \sum_{\sigma \in \mathfrak{S}} \mathbb{Q}_l^{bc_\sigma} \left(\mathbb{Q}_\sigma^{3i} + \sum_{a=1}^2 x_{c_\sigma}^a \mathbb{Q}_\sigma^{ai} \right), & \mathbb{H}_l^{bj} &= \mathbb{Q}_l^{bc_{ijk}} \left(\mathbb{Q}_{[i,j,k]}^{3j} + \sum_{a=1}^2 x_{c_{ijk}}^a \mathbb{Q}_{[i,j,k]}^{aj} \right), \\ \mathbb{H}_l^{bk} &= \sum_{\sigma \in \mathfrak{S}} \mathbb{Q}_l^{bc_\sigma} \left(\mathbb{Q}_\sigma^{3k} + \sum_{a=1}^2 x_{c_\sigma}^a \mathbb{Q}_\sigma^{ak} \right), & \mathbb{H}_l^{bm} &= \mathbb{Q}_l^{bc_{ikm}} \left(\mathbb{Q}_{[i,k,m]}^{3m} + \sum_{a=1}^2 x_{c_{ikm}}^a \mathbb{Q}_{[i,k,m]}^{am} \right). \end{aligned} \quad (5.12)$$

Note that \mathbb{H}_l^{ba} 's are diagonal matrices and hence symmetric. Because the ambient space is flat, we have

$$u^a|_b = \frac{\partial u^a}{\partial x^b} = q_l^{b,a}, \quad (5.13)$$

where $q_l^{b,a}$ denotes the a -component of \mathbf{q}_l^b . Also as $g_{ab} = \delta_{ab}$, using summation convention on index c , we can write $u_a|_b = g_{ca} u^c|_b = \delta_{ca} q_l^{b,c} = q_l^{b,a}$, and hence

$$e_{ab} = \frac{1}{2} \left(q_l^{b,a} + q_l^{a,b} \right). \quad (5.14)$$

Note that (with summation convention on indices c and d)

$$e^{ab} = g^{ac} g^{bd} e_{cd} = \delta^{ac} \delta^{bd} e_{cd} = e_{ab}. \quad (5.15)$$

So using (5.14) and (5.15) we obtain

$$\mathcal{E}^l = \frac{1}{4} \mu_l V_l \left(q_l^{b,a} + q_l^{a,b} \right) \left(q_l^{b,a} + q_l^{a,b} \right), \quad (5.16)$$

where we use summation convention on $a, b = 1, 2$, and μ_l is the value of Lamé constant μ at V_l ⁸. Alternatively, we can write (5.16) as

$$\mathcal{E}^l = \frac{1}{2} \mu_l V_l \left[(\mathbf{q}_l^1)^\top \mathbf{J} \mathbf{q}_l^1 + (\mathbf{q}_l^2)^\top \mathbf{K} \mathbf{q}_l^2 + (\mathbf{q}_l^1)^\top \mathbf{L} \mathbf{q}_l^2 \right], \quad (5.17)$$

where

$$\mathbf{J} = \begin{bmatrix} 2 & 0 \\ 0 & 1 \end{bmatrix}, \quad \mathbf{K} = \begin{bmatrix} 1 & 0 \\ 0 & 2 \end{bmatrix}, \quad \text{and} \quad \mathbf{L} = \begin{bmatrix} 0 & 0 \\ 2 & 0 \end{bmatrix}. \quad (5.18)$$

⁸Recall that μ_l can be considered as a primal 0-form.

Note that \mathbf{L} is asymmetric and as we will see in the sequel, it induces asymmetry in subsequent matrices. Substituting (5.11) into (5.17) results in

$$\mathcal{E}^l = \sum_{a,b \in \mathfrak{J}_{ijk_m}} (\mathbf{U}^a)^\top \mathbb{S}_l^{ab} \mathbf{U}^b, \quad (5.19)$$

with the matrices $\mathbb{S}_l^{ab} \in \mathbb{R}^{2 \times 2}$ given by

$$\mathbb{S}_l^{ab} = \frac{1}{2} \mu_l V_l [(\mathbb{H}_l^{1a})^\top \mathbf{J} \mathbb{H}_l^{1b} + (\mathbb{H}_l^{2a})^\top \mathbf{K} \mathbb{H}_l^{2b} + (\mathbb{H}_l^{1a})^\top \mathbf{L} \mathbb{H}_l^{2b}]. \quad (5.20)$$

Note that \mathbb{H}_l 's, \mathbf{J} , and \mathbf{K} are diagonal and so symmetric but \mathbf{L} is asymmetric, and therefore $\mathbb{S}_l^{ab} \neq (\mathbb{S}_l^{ba})^\top$, and in particular, \mathbb{S}_l^{aa} 's are not symmetric.

Next, we impose the essential boundary conditions and obtain an expression for E^d . First consider the following definitions

$$\begin{aligned} \mathfrak{N}(\sigma_a^0) &= \{\sigma^0 \in K^h \mid \exists \sigma^1 \in K^h \text{ such that } \sigma_a^0, \sigma^0 \prec \sigma^1 \text{ and } \sigma_a^0 \neq \sigma^0\}, \\ \mathfrak{E} &= \{\sigma^0 \in K^h \mid \text{Essential B.C. is imposed on } \sigma^0\}, \\ \mathfrak{E}(\sigma_a^0) &= \mathfrak{N}(\sigma_a^0) \cap \mathfrak{E}. \end{aligned} \quad (5.21)$$

Thus, $\mathfrak{N}(\sigma_a^0)$ is the set of neighbors of σ_a^0 and $\mathfrak{E}(\sigma_a^0)$ is the set of the neighbors of σ_a^0 that have essential boundary conditions. Substituting (5.19) into (5.5) yields the following expression for the discrete elastic stored energy

$$E^d = \mathbf{X}^\top \mathbf{S} \mathbf{X} + \mathbf{s} \cdot \mathbf{X} + E_e^d, \quad (5.22)$$

where $\mathbf{X} \in \mathbb{R}^{n\bar{P}_h}$ is defined in (4.7), the matrix $\mathbf{S} \in \mathbb{R}^{n\bar{P}_h \times n\bar{P}_h}$ can be written as

$$\mathbf{S} = \begin{bmatrix} \mathbb{D}^{11} & \dots & \mathbb{D}^{1\bar{P}_h} \\ \vdots & \ddots & \vdots \\ \mathbb{D}^{\bar{P}_h 1} & \dots & \mathbb{D}^{\bar{P}_h \bar{P}_h} \end{bmatrix}, \quad (5.23)$$

with

$$\mathbb{D}_{2 \times 2}^{ab} = \begin{cases} \sum_l \mathbb{S}_l^{ab}, & \text{if } b \in \mathfrak{N}(a), \\ \mathbf{0}, & \text{otherwise.} \end{cases} \quad (5.24)$$

The vector $\mathbf{s} \in \mathbb{R}^{n\bar{P}_h}$ is defined as $\mathbf{s} = \{\mathbf{d}^1, \dots, \mathbf{d}^{\bar{P}_h}\}^\top$, with

$$\mathbf{d}^a = \sum_{b \in \mathfrak{E}(a)} (\mathbf{U}^b)^\top [(\mathbb{S}_l^{ab})^\top + \mathbb{S}_l^{ba}], \quad (5.25)$$

and finally, the scalar E_e^d is given by

$$E_e^d = \sum_{a \in \mathfrak{E}} \sum_l (\mathbf{U}^a)^\top \mathbb{S}_l^{aa} \mathbf{U}^a. \quad (5.26)$$

The summation on l in (5.24) denotes summation over all those regions whose elastic energies are affected by the displacements of vertices a and b . Equation (5.26) has a similar interpretation. The matrix \mathbf{S} is not symmetric, in general, and the vector \mathbf{s} is zero if boundary vertices have zero displacements. Because both \mathbf{S} and \mathbf{S}^\top appear in the Euler-Lagrange equations, the governing equations remain symmetric in the sense that reciprocity holds. Also similar to K_e^d defined in (5.2), E_e^d does not contribute to the Euler-Lagrange equations either. Finally, note that there are other possible choices for writing a discrete elastic energy. In the next section, we use the discrete kinetic and elastic stored energies to write a discrete Lagrangian and obtain the Euler-Lagrange equations for linearized incompressible elasticity.

5.3 Discrete Euler-Lagrange Equations

In this section we use Hamilton's principle in the space of divergence-free displacements to obtain the Euler-Lagrange equations for the unknown \mathbf{X} . As in the continuous case that was discussed in §2.2.1, we do not use Lagrange multipliers to impose the incompressibility constraint. Instead, we confine the solution space to the divergence-free displacements and gradient of pressure appears naturally.

Similar to the Lagrangian in the continuous case, we define the discrete Lagrangian as

$$L^d = K^d - V^d, \quad (5.27)$$

where $V^d = E^d - B^d - T^d$, with B^d and T^d denoting the work of body forces and tractions at boundary nodes, respectively. We model a body force with a primal vector field. Let \mathbf{B}^i be the body force at vertex i . Then, we have

$$B^d = \sum_{i=1}^{P_h} m^i \mathbf{B}^i \cdot \mathbf{U}^i = \mathbf{b} \cdot \mathbf{X} + B_e^d, \quad (5.28)$$

where $m^i = \rho_i |\star \sigma_i^0|$, is the mass of the dual cell $\star \sigma_i^0$ and $\mathbf{b} \in \mathbb{R}^{n\bar{P}_h}$ is defined as $\mathbf{b} = \{\mathbf{b}^1, \dots, \mathbf{b}^{\bar{P}_h}\}^\top$, with $\mathbf{b}^i = m^i \mathbf{B}^i$, and

$$B_e^d = \sum_{i=\bar{P}_h+1}^{P_h} m^i \mathbf{B}^i \cdot \mathbf{U}^i. \quad (5.29)$$

Note that similar to the previous section, we order the primal vertices such that $\{\sigma_i^0\}_{i=1}^{\bar{P}_h}$ and $\{\sigma_i^0\}_{i=\bar{P}_h+1}^{P_h}$ denote the primal vertices without and with essential boundary conditions, respectively. Let us define

$$T^d = \mathbf{t} \cdot \mathbf{X}, \quad (5.30)$$

where the vector $\mathbf{t} \in \mathbb{R}^{n\bar{P}_h}$ is defined as $\mathbf{t} = \{\mathbf{t}^1, \dots, \mathbf{t}^{\bar{P}_h}\}$, with $\mathbf{t}^i = \mathbf{0}$, if the traction at σ_i^0 is zero. Note that we assume that the set of vertices with essential boundary conditions and the set of vertices with natural boundary conditions are disjoint. Therefore, the specified displacements do not contribute to T^d . Substituting (5.3), (5.22), (5.28), and (5.30) into (5.27) results in

$$L^d = \frac{1}{2} \dot{\mathbf{X}}^\top \mathbf{M} \dot{\mathbf{X}} - \mathbf{X}^\top \mathbf{S} \mathbf{X} + \mathbf{F} \cdot \mathbf{X} + L_e^d, \quad (5.31)$$

where

$$\mathbf{F} = -\mathbf{s} + \mathbf{b} + \mathbf{t}, \quad L_e^d = K_e^d - E_e^d + B_e^d. \quad (5.32)$$

Let the variational field of \mathbf{X} be a 1-parameter family of divergence-free vector fields \mathbf{X}_ϵ that satisfy the essential boundary conditions and

$$\mathbf{X}_0 = \mathbf{X}, \quad \left. \frac{d}{d\epsilon} \right|_{\epsilon=0} \mathbf{X}_\epsilon = \delta \mathbf{X}. \quad (5.33)$$

Note that \mathbf{X}_ϵ satisfies (4.6), i.e.

$$\mathbb{I}^h \mathbf{X}_\epsilon = \mathbf{u}^h, \quad (5.34)$$

and therefore

$$\mathbb{I}^h \delta \mathbf{X} = \mathbf{0}, \quad (5.35)$$

which means that $\delta \mathbf{X} \in \text{Ker}(\mathbb{I}^h)$. Hamilton's principle tells us that

$$\delta \int_{t_1}^{t_2} L^d dt = \left. \frac{d}{d\epsilon} \right|_{\epsilon=0} \int_{t_1}^{t_2} L_\epsilon^d dt = 0. \quad (5.36)$$

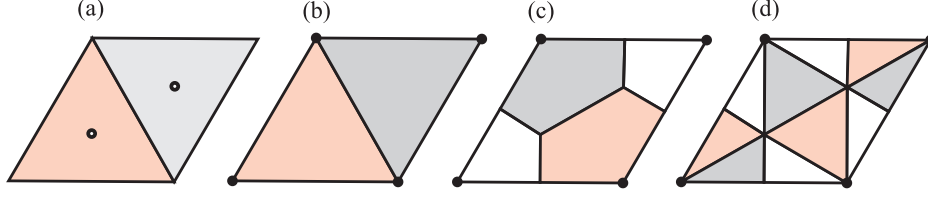


Figure 5.3: Discrete solution spaces: (a) \mathbb{P}_0 over primal meshes for the pressure field, (b) \mathbb{P}_1 over primal meshes for the displacement field in the incompressibility constraint, (c) \mathbb{P}_0 over dual meshes for the displacement field for approximating the kinetic energy, and (d) \mathbb{P}_1 over support volumes for the displacement field for approximating the elastic energy.

Using (5.31) we can write

$$\begin{aligned}
\delta \int_{t_1}^{t_2} L^d dt &= \frac{d}{d\epsilon} \Big|_{\epsilon=0} \int_{t_1}^{t_2} \left(\frac{1}{2} \dot{\mathbf{X}}_\epsilon^\top \mathbf{M} \dot{\mathbf{X}}_\epsilon - \mathbf{X}_\epsilon^\top \mathbf{S} \mathbf{X}_\epsilon + \mathbf{F} \cdot \mathbf{X}_\epsilon + L_e^d \right) dt \\
&= \int_{t_1}^{t_2} \left[\dot{\mathbf{X}}^\top \mathbf{M} \left(\frac{d}{dt} \delta \mathbf{X} \right) - \mathbf{X}^\top (\mathbf{S} + \mathbf{S}^\top) \delta \mathbf{X} + \mathbf{F} \cdot \delta \mathbf{X} \right] dt \\
&= - \int_{t_1}^{t_2} \left[\mathbf{M} \ddot{\mathbf{X}} + (\mathbf{S} + \mathbf{S}^\top) \mathbf{X} - \mathbf{F} \right] \cdot \delta \mathbf{X} dt = 0,
\end{aligned} \tag{5.37}$$

where we used symmetry of the matrix \mathbf{M} , the integration by parts for simplifying the kinetic energy contribution, and the assumption that $\delta \mathbf{X}$ is a proper variation, i.e., $\delta \mathbf{X} = \mathbf{0}$ at both t_1 and t_2 . Because the integrand of (5.37) is a continuous function of time and t_1 and t_2 are arbitrary, we obtain

$$\left[\mathbf{M} \ddot{\mathbf{X}} + (\mathbf{S} + \mathbf{S}^\top) \mathbf{X} - \mathbf{F} \right] \cdot \delta \mathbf{X} = 0. \tag{5.38}$$

Note that we can write

$$\mathbb{R}^{n\bar{P}_h} = \text{Ker}(\mathbb{I}^h) \oplus \text{Ker}(\mathbb{I}^h)^\perp, \tag{5.39}$$

and since $\delta \mathbf{X} \in \text{Ker}(\mathbb{I}^h)$, from (5.38) we conclude that

$$\mathbf{M} \ddot{\mathbf{X}} + (\mathbf{S} + \mathbf{S}^\top) \mathbf{X} - \mathbf{F} = \mathbf{\Lambda}, \tag{5.40}$$

where $\mathbf{\Lambda} \in \text{Ker}(\mathbb{I}^h)^\perp$.

Remark. In the smooth case, we observed that confining the variations to the divergence-free vector fields results in the appearance of pressure gradient in the balance of linear momentum. As the vector $\mathbf{\Lambda}$ appears in the discrete governing equations through a similar procedure, it is reasonable to expect that this vector should somehow be related to discrete pressure gradient. As a matter of fact, the vector $\mathbf{\Lambda} \in \mathbb{R}^{n\bar{P}_h}$ can be written as

$$\mathbf{\Lambda} = \left\{ \mathbf{\Lambda}^1, \dots, \mathbf{\Lambda}^{\bar{P}_h} \right\}^\top, \tag{5.41}$$

where $\mathbf{\Lambda}^i \in \mathbb{R}^n$ can be thought as the value of the gradient of pressure at the primal vertex σ_i^0 . Although we do not conduct a convergence analysis to show that the pressure field that is obtained by this assumption converges to the smooth pressure field, our numerical examples in the next section demonstrate that this assumption is valid. On the other hand, this correspondence suggests that pressure should be a dual zero-form because $\nabla p = (d\mathbf{p})^\sharp$. This is a geometric justification for the known fact that using different function spaces for displacement and pressure is crucial in incompressible linearized elasticity [3, 4]. Also note that we do not obtain the pressure gradient for vertices with essential boundary conditions.

Recall that $\text{Ker}(\mathbb{I}^h)^\perp$ is the orthogonal complement of the null space of \mathbb{I}^h , which is the row space of \mathbb{I}^h , i.e., the space spanned by the rows of \mathbb{I}^h . To obtain $\mathbf{\Lambda}$, note that from the rank-nullity theorem, one can write

$$\dim(\text{Ker}(\mathbb{I}^h)^\perp) = n\bar{P}_h - \text{nullity}(\mathbb{I}^h) = \text{rank}(\mathbb{I}^h) = R. \tag{5.42}$$

Let $\{\mathbf{z}^1, \dots, \mathbf{z}^R\}$ be a basis for $\text{Ker}(\mathbb{I}^h)^\perp$. Then, we have

$$\mathbf{\Lambda}(t) = \sum_{i=1}^R \Lambda_i(t) \mathbf{z}^i, \quad (5.43)$$

where the time-dependent functions Λ_i 's are unknowns to be determined. Thus, we have the following discrete governing equations for the unknowns \mathbf{X} and Λ_i 's:

$$\mathbf{M}\ddot{\mathbf{X}} + (\mathbf{S} + \mathbf{S}^\top)\mathbf{X} - \mathbf{F} = \sum_{i=1}^R \Lambda_i \mathbf{z}^i, \quad (5.44)$$

$$\mathbb{I}^h \mathbf{X} = \mathbf{u}^h. \quad (5.45)$$

The number of unknowns is $n\bar{P}_h + R$ and since $\text{rank}(\mathbb{I}^h) = R$, we conclude that \mathbb{I}^h has R independent rows (columns) and thus (5.45) has R independent equations and so the number of independent equations becomes $n\bar{P}_h + R$, which is equal to the number of unknowns. Therefore, one can solve (5.44) and obtain the displacement field and the pressure gradient.

Remark. The difference between our approach for deriving (5.44) and (5.45) and that of the FE method is as follows. As we mentioned in §4, (5.45) is equivalent to a Lagrange finite element approximation, where the pressure field is approximated by \mathbb{P}_0 polynomials over the primal mesh and the displacement field is approximated by piecewise linear \mathbb{P}_1 polynomials over the primal mesh. On the other hand, we used two different spaces for the displacement field for writing (5.44), see Fig. 5.3. For discretizing the kinetic energy, the displacement field is discontinuous and is approximated by \mathbb{P}_0 polynomials over the dual mesh. However, for discretizing the elastic energy, it is continuous and is approximated by \mathbb{P}_1 polynomials over (part of) the support volumes.

Remark. (Incompressible linear elastostatics) For incompressible linearized elastostatics, the displacements and pressures are time independent, and therefore (5.44) and (5.45) are equivalent to

$$\mathbb{K}_{(n\bar{P}_h + D_h) \times (n\bar{P}_h + R)} \mathbb{X}_{(n\bar{P}_h + R) \times 1} = \mathbb{F}_{(n\bar{P}_h + D_h) \times 1}, \quad (5.46)$$

where

$$\mathbb{K} = \begin{bmatrix} (\mathbf{S} + \mathbf{S}^\top)_{n\bar{P}_h \times n\bar{P}_h} & -\mathbf{Z}_{n\bar{P}_h \times R} \\ \mathbb{I}_{D_h \times n\bar{P}_h}^h & \mathbf{0}_{D_h \times R} \end{bmatrix}, \quad (5.47)$$

with the i th column of \mathbf{Z} equal to \mathbf{z}^i for $i = 1, \dots, R$. Also by defining $\boldsymbol{\lambda} = \{\Lambda_1, \dots, \Lambda_R\}^\top \in \mathbb{R}^R$, the vectors \mathbb{X} and \mathbb{F} can be written as

$$\mathbb{X} = \begin{Bmatrix} \mathbf{X} \\ \boldsymbol{\lambda} \end{Bmatrix} \in \mathbb{R}^{n\bar{P}_h + R}, \quad \mathbb{F} = \begin{Bmatrix} \mathbf{F} \\ \mathbf{u}^h \end{Bmatrix} \in \mathbb{R}^{n\bar{P}_h + D_h}. \quad (5.48)$$

5.4 Discrete Pressure Field

Equations (5.44) and (5.45) enable us to obtain the displacement field of linear incompressible elasticity together with the pressure gradient $\mathbf{\Lambda}$. The next step is to calculate stresses. Note that we do not define a notion of discrete stress and, instead, we define stresses on subregions with constant strains, cf. §5.2. Therefore, we define the stress to be

$$\sigma^{ab} = 2\mu e^{ab} - p g^{ab}, \quad (5.49)$$

on each shaded region of Fig. 5.2. Using (5.14) and (5.15), the stress of the subregion l can be written as

$$\sigma_l^{ab} = \mu_l \left(q_l^{a,b} + q_l^{b,a} \right) - p_l \delta^{ab}. \quad (5.50)$$

Thus, we need to calculate the value of pressure on each dual vertex. The number of unknown pressures is D_h . Let $\{p^1, \dots, p^{D_h}\}$ denote the value of unknown pressures at dual vertices. We need to obtain D_h independent equations from the pressure gradient $\mathbf{\Lambda}$ to be able to specify the pressure. One way to do so is to use the discrete Laplace-Beltrami operator. This is explained in the following example.

Example 5.1. Consider the planar mesh of Fig. 4.4 once again. Let p be a dual 0-form on this mesh representing the pressure and suppose p^{123} denotes $\langle p, \star[1, 2, 3] \rangle$, etc. We know that Δp is also a dual 0-form. Let us define the vector $\mathbf{p} \in \mathbb{R}^6$ as

$$\mathbf{p} = \{p^{132}, p^{143}, p^{154}, p^{165}, p^{176}, p^{127}\}^\top. \quad (5.51)$$

One can use (3.21) to calculate Δp . On the other hand, one can obtain Δp using the pressure gradient $\mathbf{\Lambda}$. Suppose, for example, that the vertices 2 and 3 have essential boundary conditions. Thus, pressure gradient obtained from (5.44) lies in \mathbb{R}^{10} and Δp is equal to the divergence of $\mathbf{\Lambda}$. To calculate the discrete pressure field, we need to obtain the discrete pressure gradient $\mathbb{G}_p \in \mathbb{R}^{14}$, which is a primal vector field. To this end, we need to assign a pressure gradient to those vertices that have essential boundary conditions. This can be done by assuming that pressure gradient of these vertices are equal to those of their closest interior primal vertices. This way, using $\mathbf{\Lambda}$, we can obtain the pressure gradient $\mathbb{G}_p \in \mathbb{R}^{14}$. Now we equate the expressions for Δp obtained using the previous two approaches. This gives

$$\mathbb{L}_{6 \times 6} \mathbf{p} = \bar{\mathbb{I}}_{6 \times 14} \mathbb{G}_p, \quad (5.52)$$

where $\bar{\mathbb{I}}$ is given in (4.19) and

$$\mathbb{L} = \begin{bmatrix} r_{1,2}+r_{1,3}+r_{2,3} & -r_{1,3} & 0 & 0 & 0 & -r_{1,2} \\ -r_{1,3} & r_{1,3}+r_{1,4}+r_{3,4} & -r_{1,4} & 0 & 0 & 0 \\ 0 & -r_{1,4} & r_{1,4}+r_{1,5}+r_{4,5} & -r_{1,5} & 0 & 0 \\ 0 & 0 & -r_{1,5} & r_{1,5}+r_{1,6}+r_{5,6} & -r_{1,6} & 0 \\ 0 & 0 & 0 & -r_{1,6} & r_{1,6}+r_{1,7}+r_{6,7} & -r_{1,7} \\ -r_{1,2} & 0 & 0 & 0 & -r_{1,7} & r_{1,7}+r_{1,2}+r_{2,7} \end{bmatrix}, \quad (5.53)$$

with

$$r_{i,j} = \frac{|[i,j]|}{|\star[i,j]|}. \quad (5.54)$$

The right-hand side of (5.52) is a discrete analogue of $\Delta = \text{div} \circ \text{grad}$. Note that here \mathbb{L} is symmetric and invertible. Therefore, we are able to obtain a unique dual 0-form p .

Let us consider a planar mesh K_h . Fig. 4.2 shows part of this mesh. We define a symmetric matrix $\mathbb{L}^h \in \mathbb{R}^{\mathbb{D}_h \times \mathbb{D}_h}$ as follows. Each row of \mathbb{L}^h corresponds to a dual vertex of K_h . All the elements in each row are zero except the diagonal elements and the ones that correspond to the dual vertices that are joined to the reference dual vertex by a dual 1-simplex. For example, in Fig. 4.2, nonzero components of the row that corresponds to $\star[j, l, k]$ are those that correspond to $\star[j, l, k]$, $\star[j, o, l]$, $\star[l, q, k]$, and $\star[r, j, k]$. Let us denote these components of \mathbb{L}^h by $\mathbb{L}_{jlk,jlk}$, $\mathbb{L}_{jlk,jol}$, $\mathbb{L}_{jlk,lqk}$, and $\mathbb{L}_{jlk,rjk}$, respectively. Then, we have

$$\mathbb{L}_{jlk,jlk} = r_{l,k} + r_{k,j} + r_{j,l}, \quad \mathbb{L}_{jlk,jol} = -r_{j,l}, \quad \mathbb{L}_{jlk,lqk} = -r_{l,k}, \quad \mathbb{L}_{jlk,rjk} = -r_{k,j}. \quad (5.55)$$

Note that if $[j, l, k]$ is on the boundary as shown in Fig. 5.4, then the only nonzero components are $\mathbb{L}_{jlk,jlk}$, $\mathbb{L}_{jlk,jol}$, and $\mathbb{L}_{jlk,lqk}$, which are defined as above. Note also that by construction, the matrix \mathbb{L}^h is symmetric. The sum of the components of the row corresponding to an internal primal n -simplex is zero while the same sum for rows that correspond to boundary n -simplices is not zero. As we will see in the following theorem, as a result of this specific structure, the symmetric matrix \mathbb{L}^h is nonsingular and because Δp can be calculated using this matrix, the dual Laplace-Beltrami operator is injective. Note that the primal Δ operator is not injective. The reason for this is that the dual coboundary operator is not the same as the geometric boundary of a dual cell, see (3.12) and (3.21), and the corresponding discussions.

Theorem 5.1. *Let K_h be a planar well-centered primal mesh such that $|K_h|$ is a simply-connected set. Then, the matrix $\mathbb{L}^h \in \mathbb{R}^{\mathbb{D}_h \times \mathbb{D}_h}$ is nonsingular.*

Proof: The proof of this theorem is similar to that of Theorem 4.1. Using the fact that K_h is shellable, one can use induction and the specific structure of the matrix \mathbb{L} to complete the proof. ■

Let the vector $\mathbf{p} \in \mathbb{R}^{\mathbb{D}_h}$ denote the pressure p on K_h , i.e., the i th component of \mathbf{p} is $p^i = \langle p, \hat{\sigma}_i^0 \rangle$, where $\hat{\sigma}_i^0$

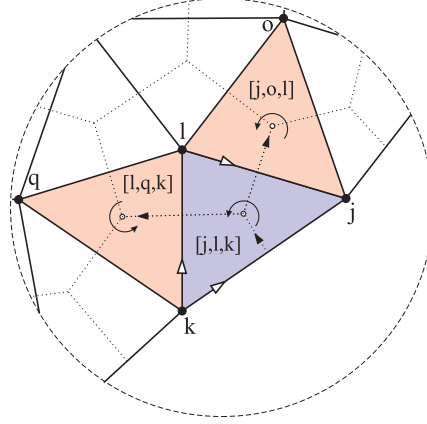


Figure 5.4: Part of a primal mesh and its associated dual mesh. The 2-simplex $[j, l, k]$ lies on the boundary.

is the i th dual vertex. Then, one can use \mathbb{L}^h to calculate Δp . Alternatively, Δp can be calculated using the pressure gradient $\mathbb{G}_p \in \mathbb{R}^{n_{P_h}}$, which is a vector that has the same components as $\mathbf{\Lambda} \in \mathbb{R}^{n_{P_h}}$ at vertices without essential boundary conditions. Those components that are associated with vertices with essential boundary conditions are chosen to be equal to the pressure gradient of the closest internal primal vertex. For example, suppose in Fig. 5.4, vertex k has essential boundary conditions and the closest internal vertex to k is l . Then, pressure gradient at vertex k is assumed to be equal to the pressure gradient at l .⁹ Then, equating Δp 's obtained using the above two approaches we obtain

$$\mathbb{L}^h \mathbf{p} = \bar{\mathbb{I}}^h \mathbb{G}_p, \quad (5.56)$$

and because \mathbb{L}^h is nonsingular one can solve (5.56) and obtain the pressure on each dual vertex. However, our numerical experiments show that the direct use of (5.56) does not yield satisfactory results for pressure and this is not unusual as we have not imposed the natural boundary conditions on each primal 2-cell with such boundary conditions yet. Recall that if τ^a denotes the a -component of the traction $\boldsymbol{\tau}$, then using the summation convention on index b , we can write

$$\tau^a = \sigma^a_b n^b = (2\mu e^a_b - p g^a_b) n^b, \quad (5.57)$$

where n^b is the b -component of the unit outward normal vector at the natural boundary. Now suppose that in Fig. 5.4, the 2-cell $[j, l, k]$ lies on the natural boundary. Then, using (5.50) and (5.57) we can write

$$\tau^a_{kj} = \left[\mu_{jlk} \left(q_{jlk}^{a,b} + q_{jlk}^{b,a} \right) - p_{jlk} \delta^{ab} \right] n^b_{kj}, \quad (5.58)$$

where we assume summation convention on index b . Using (5.58) we can determine the pressure at all the 2-cells with natural boundary conditions. Next, we omit the rows that correspond to those 2-cells with natural boundary conditions in (5.56) and move all the terms containing the known values of the pressure to the right-hand side of the remaining equations. This way, from (5.56) we obtain the required number of equations to determine pressure at all the dual vertices. Finally, one can use (5.50) to calculate the stress on each dual subregion.

6 Numerical Examples

To demonstrate the efficiency and robustness of our geometric method, in this section we consider the following two 2-dimensional benchmark problems: a cantilever beam subjected to a parabolic end load and Cook's membrane.

⁹If there are more than one closest vertices, one can associate the average pressure to vertex k .

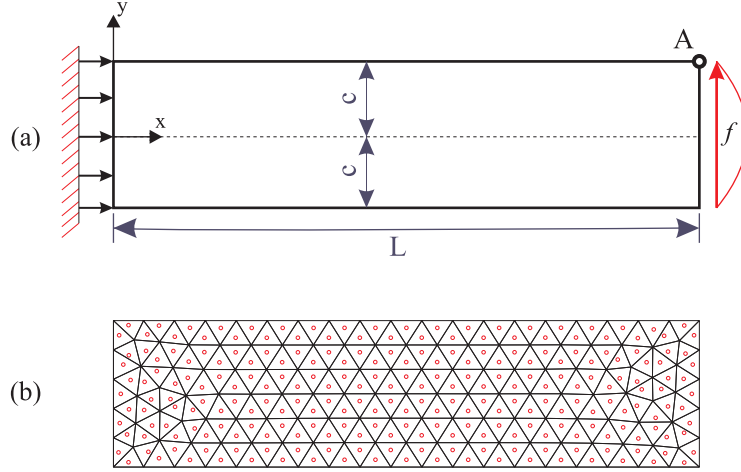


Figure 6.1: Cantilever beam: (a) Geometry, boundary conditions, and loading, (b) a well-centered primal mesh with \circ denoting the circumcenter of each primal 2-cell.

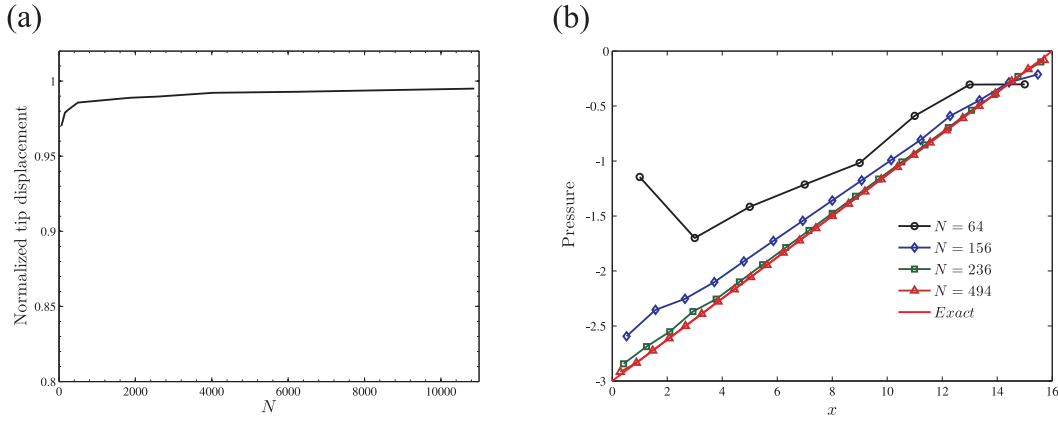


Figure 6.2: Cantilever beam: (a) Convergence of the normalized displacement of the tip point A (ratio of the numerically-calculated and exact displacements). N is the number of primal 2-cells of the mesh. (b) Pressure of the dual vertices that correspond to the primal 2-cells that are on the bottom of the beam.

Cantilever beam. As our first example, we consider a planner cantilever beam shown in Fig. 6.1 that has a closed-form solution for its displacements field [65]. The parabolic load per unit length at the right boundary is given by $f(y) = \frac{F}{2I}(c^2 - y^2)$, where $I = 2c^3/3$. Thus, the total shear load on the right boundary is F . Now, we consider the analytical solution for a beam under this load given by

$$u_x = \frac{(1 - \nu^2)Fy}{6EI} \left(3x^2 - 6Lx + \frac{\nu y^2}{1 - \nu} \right) - \frac{Fy}{6I\mu} (y^2 - 3c^2), \quad (6.1)$$

$$u_y = \frac{(1 - \nu^2)F}{6EI} \left[\frac{3\nu(L - x)y^2}{1 - \nu} + 3Lx^2 - x^3 \right], \quad (6.2)$$

and impose the displacements at $x = 0$. The divergence of the displacement field reads

$$\operatorname{div} \mathbf{u} = \frac{1}{EI} (1 + \nu)(1 - 2\nu)F(x - L)y, \quad (6.3)$$

and hence, for $\nu = 0.5$ we have $\operatorname{div} \mathbf{u} = \mathbf{0}$. Note that if $\nu = 0.5$, then as we explained in Remark 2.2.1, the above displacements also satisfy the equations of incompressible linearized elasticity. For this case, pressure is given

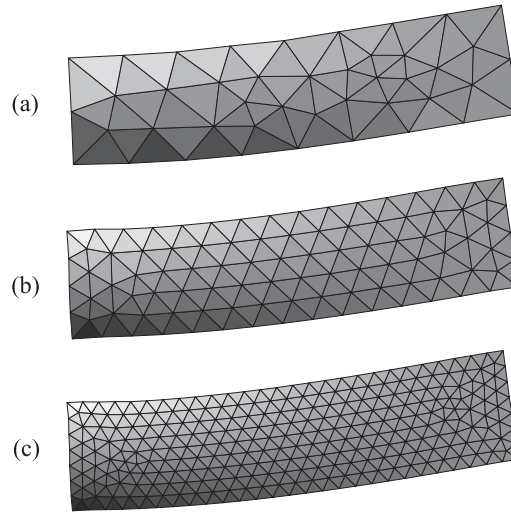


Figure 6.3: The pressure field for the beam problem for meshes with (a) $N = 64$, (b) $N = 156$, (c) $N = 494$, where N is the number of primal 2-cells of the mesh.

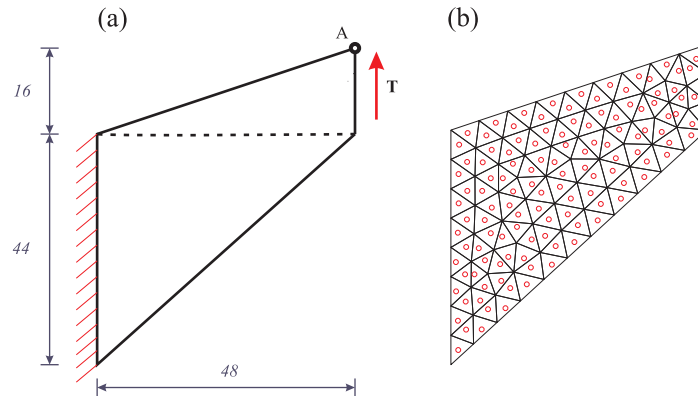


Figure 6.4: Cook's membrane: (a) geometry, boundary conditions, and loading, (b) a well-centered mesh with $N = 123$ primal 2-cells with \circ denoting the circumcenter of each primal 2-cell.

by

$$p(x, y) = -\frac{F(x-L)y}{2I}. \quad (6.4)$$

We assume the following parameters: $L = 16$, $c = 2$, $F = 1$, $E = 10^7$, and $\nu = 0.5$. We show one of the primal meshes with $N = 236$ primal 2-cells in Fig. 6.1(b). We increase the number of primal 2-cells and study the convergence of the solutions. In Fig 6.2(a), we plot the normalized vertical displacement of the tip point A defined as U_y^A/u_y^A , where U_y^A and u_y^A denote the vertical displacement of point A obtained by our structure-preserving scheme and the exact solution, respectively. We see that the numerical solutions converge to the exact solution. Moreover, we observe a smooth pressure field for the beam. As an example, in Fig. 6.2(b) we show the variation of pressure at the bottom of the beam ($y = -c$) in the x -direction and again we observe that pressure converges to its exact value. We plot the pressure field over different primal meshes with exaggerated deformations in Fig. 6.3. The pressure field is free from checkerboarding and becomes smoother and smoother upon mesh refinement.

Cook's membrane. Now we consider the Cook's membrane problem, which is a standard benchmark problem that has been used in the past to investigate the incompressible and near-incompressible solutions under combined bending and shear [4, 30]. Fig. 6.4 depicts the geometry, boundary conditions, and loading of the

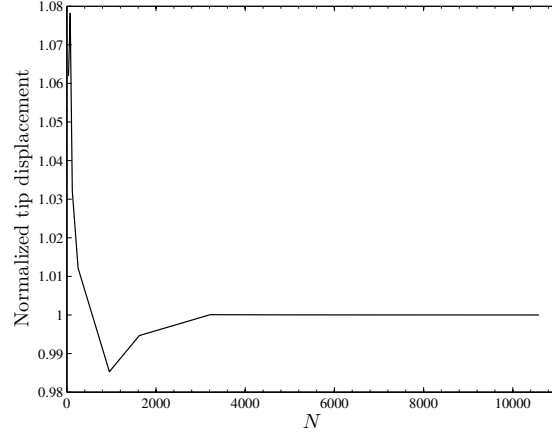


Figure 6.5: Convergence of the normalized displacement of the tip point A of the Cook's membrane. N is the number of primal 2-cells of the mesh.

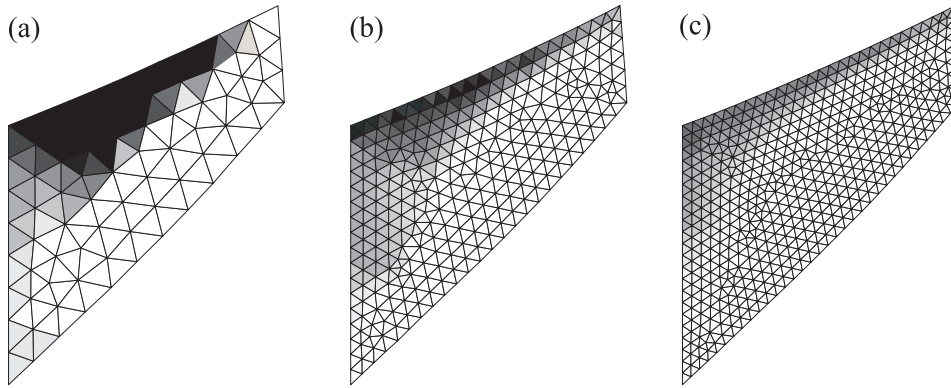


Figure 6.6: The pressure field for the Cook's membrane for meshes with (a) $N = 123$, (b) $N = 530$, (c) $N = 955$, where N is the number of primal 2-cells of the mesh.

problem together with a well-centered mesh with $N = 123$ primal 2-cells. The left boundary is fully clamped and the right boundary is subjected to a distributed shearing load of magnitude $T = 6.25$ per unit length (a total vertical force of 100 is imposed on the right boundary). The material is assumed to be homogeneous with the parameters $E = 250$ and $\nu = 0.5$. Now we study the variations of the vertical displacement of the tip point A upon mesh refinement. The result is plotted in Fig. 6.5 that shows the convergence of the normalized displacements by increasing the number of primal 2-cells, N . Note that we use the limit value of the numerically-calculated displacement $U_y^A = 4.2002$ for normalization of displacements in this figure. Finally, we observe that our structure-preserving scheme is free of checkerboarding as is clearly seen in Fig. 6.6. In this figure, we plot the pressure field over deformed configuration of Cook's membrane. We see that pressure field becomes smoother and smoother upon mesh refinement. Also note that the rate of convergence of the results in our numerical examples is comparable with those of finite element mixed formulations [4, 30].

7 Concluding Remarks

In this paper, we presented a discrete geometric structure-preserving numerical scheme for incompressible linearized elasticity. We proved that the governing equations of finite and linearized incompressible elasticity can be obtained using Hamilton's principle and Hodge decomposition theorem without using Lagrange multipliers.

We used ideas from algebraic topology, exterior calculus, and discrete exterior calculus to develop a discrete geometric theory for linearized elasticity. We considered the discrete displacement field as our primary unknown

and characterized the space of divergence-free discrete displacements as the solution space. Note that instead of heuristically defining the discrete displacement field and its divergence as a discretization of a smooth vector field and smooth divergence operator, we assume the discrete displacement field to be a discrete primal vector field and use the definition of discrete divergence using DEC techniques. Therefore, we preserve the geometric structure of the smooth problem by considering discrete quantities that have the same geometric structure as their smooth counterparts. This guarantees that the method remains free of numerical artifacts as we remain in the correct discrete space unlike the standard finite element and finite difference schemes.

Finally, motivated by the Lagrangian structure of the smooth case, we defined a discrete Lagrangian and used Hamilton's principle in the space of discrete divergence-free displacement fields to obtain the governing equations of the discrete theory. We observed that the discrete gradient of pressure appears naturally in the governing equations. We used the discrete Laplace-Beltrami operator to determine the pressure field, which is assumed to be a dual 0-form. We then considered some numerical examples and observed that our discretization scheme is free of numerical artifacts, e.g. checkerboarding of pressure. Based on the rate of convergence of the results of the numerical examples, our method is comparable with finite element mixed formulations [4, 30]. We observed that by choosing the displacement field to be a primal vector field, pressure is a dual 0-form; this geometrically justifies the known fact that using different function spaces for displacement and pressure is helpful in the incompressible regime. Also note that our method can be used for analyzing multiply-connected bodies as well.

The smooth weak form of the incompressible elasticity is well-posed. However, it is a well-known fact that the discretization of the weak form is well-posed if and only if the discrete spaces for the displacement and pressure fields are compatible [3]. For example, a $\mathbb{P}_0/\mathbb{P}_1$ Lagrange finite element approximation for the displacement/pressure field is not well-posed. This low order approximation is not well-posed even when using the diamond element approach [4]. Although we do not present any proof, our numerical results suggest that the discrete weak form is well-posed for our choices of the discrete solution spaces. This also suggests that choices that are naturally imposed by the geometry of a problem can be nontrivial and hard to see using other approaches.

The structure of linearized elasticity is similar to that of perfect fluids in the sense that both need a fixed mesh. However, finite elasticity requires the material description of motion. This means that one needs the time evolution of the initial simplicial complex of the reference configuration. However, this evolving mesh would not remain a simplicial complex, in general, and hence the extension of this work to the case of finite elasticity is not straightforward. Also the convergence issues are not considered in this work. Applications to fluid mechanics and finite elasticity and studying convergence issues will be the subjects of future communications.

Acknowledgments. We benefited from a discussion with Marino Arroyo that helped us understand the difference between our approach and the finite element method. We also thank the anonymous referees for their comments that led to an improvement of the presentation of our work. This research was partially supported by AFOSR – Grant No. FA9550-10-1-0378 and FA9550-12-1-0290 and NSF – Grant No. CMMI 1042559 and CMMI 1130856.

References

- [1] J. P. Whiteley. Discontinuous Galerkin finite element methods for incompressible non-linear elasticity. *Comput. Methods Appl. Mech. Engrg.*, 198:3464–3478, 2009.
- [2] A. Yavari. A geometric theory of growth mechanics. *J. Non. Sci.*, 20:781–830, 2010.
- [3] A. Ern and J. Guermond. *Theory and Practice of Finite Elements*. Springer-Verlag, New York, 2004.
- [4] P. Hauret, E. Kuhl, and M. Ortiz. Diamond elements: A finite element/discrete-mechanics approximation scheme with guaranteed optimal convergence in incompressible elasticity. *Int. J. Numer. Meth. Engrg.*, 72: 253–294, 2007.
- [5] F. Auricchio, L. da Veiga Beirao, C. Lovadina, and A. Reali. The importance of the exact satisfaction of the incompressibility constraint in nonlinear elasticity: mixed FEMs versus NURBS-based approximations. *Comput. Methods Appl. Mech. Engrg.*, 199:314–323, 2010.

- [6] I. Babuška and M. Suri. On locking and robustness in the finite element method. *SIAM J. Numer. Anal.*, 29:1261–1293, 1992.
- [7] M. Suri. Analytical and computational assessment of locking in the hp finite element method. *Comput. Meth. Appl. Mech. Engrg.*, 133:347–371, 1996.
- [8] L. Scott and M. Vogelius. Norm estimates for a maximal right inverse of the divergence operator in spaces of piecewise polynomials. *Math. Model. Numer. Anal.*, 19:111–143, 1985.
- [9] P. Hansbo and M. G. Larson. Discontinuous Galerkin methods for incompressible and nearly incompressible elasticity by Nitsche’s method. *Comput. Meth. Appl. Mech. Engrg.*, 191:1895–1908, 2002.
- [10] L. J. Bridgeman and T. P. Wihler. Stability and a posteriori error analysis of discontinuous Galerkin methods for linearized elasticity. *Comput. Meth. Appl. Mech. Engrg.*, 200:1543–1557, 2011.
- [11] R. Liu, M. F. Wheeler, and C.N. Dawson. A three-dimensional nodal-based implementation of a family of discontinuous Galerkin methods for elasticity problems. *Comput. Struct.*, 87:141–150, 2009.
- [12] T. P. Wihler. Locking-free DGFEM for elasticity problems in polygons. *IMA J. Num. Anal.*, 24:45–75, 2004.
- [13] R. S. Falk. Nonconforming finite element methods for the equations of linear elasticity. *Math. Comp.*, 57:529–550, 1991.
- [14] L. Wang and H. Qi. A locking-free scheme of nonconforming rectangular finite element for the planar elasticity. *J. Comp. Math.*, 22:641–650, 2004.
- [15] S. Chen, G. Ren, and S. Mao. Second-order locking-free nonconforming elements for planar linear elasticity. *J. Comp. Appl. Math.*, 233:2534–2548, 2010.
- [16] J. Simo and M. Rifai. A class of assumed strain method and the methods of incompatible modes. *Int. J. Num. Methods Eng.*, 29:1595–1638, 1990.
- [17] E. Kasper and R. Taylor. A mixed-enhanced strain method. Part I: Geometrically linear problems. *Comput. Struct.*, 75:237–250, 2000.
- [18] U. Brink and E. P. Stephan. Adaptive coupling of boundary elements and mixed finite elements for incompressible elasticity. *Num. Meth. Part. Dif. Eq.*, 17:79–92, 2001.
- [19] M. Cervera, M. Chiumenti, Q. Valverde, and C. Agelet de Saracibar. Mixed linear/linear simplicial elements for incompressible elasticity and plasticity. *Comput. Methods Appl. Mech. Engrg.*, 192:5249–5263, 2003.
- [20] Y. Shen and A. J. Lew. A family of discontinuous Galerkin mixed methods for nearly and perfectly incompressible elasticity. *ESAIM: Math. Model. Num. Anal.*, 46:1003–1028, 2012.
- [21] P. Houston, D. Schotzau, and T. P. Wihler. An hp-adaptive mixed discontinuous Galerkin FEM for nearly incompressible linear elasticity. *Comput. Methods Appl. Mech. Engrg.*, 195:3224–3246, 2006.
- [22] T. J. R. Hughes. *The Finite Element Method*. Prentice-Hall, Englewood Cliffs, NJ, 2000.
- [23] D. S. Malkus and T. J. R. Hughes. Mixed finite element methods - Reduced and selective integration techniques: A unification of concepts. *Comput. Methods Appl. Mech. Eng.*, 15:63–81, 1978.
- [24] P. Areias and K. Matous. Stabilized four-node tetrahedron with nonlocal pressure for modeling hyperelastic materials. *J. Numer. Methods Eng.*, 76:1185–1201, 2008.
- [25] J. Bonet and A. J. Burton. A simple average nodal pressure tetrahedral element for incompressible and nearly incompressible dynamic explicit applications. *Comm. Num. Meth. Eng.*, 14:437–449, 1998.
- [26] P. Krysl and B. Zhu. Locking-free continuum displacement finite elements with nodal integration. *Int. J. Numer. Methods Eng.*, 76:1020–1043, 2008.

- [27] G. N. Gatica, L. F. Gatica, and E. P. Stephan. A dual-mixed finite element method for nonlinear incompressible elasticity with mixed boundary conditions. *Comput. Methods Appl. Mech. Engrg.*, 196:3348–3369, 2007.
- [28] T. Belytschko, Y. Y. Lu, and L. Gu. Element-free Galerkin methods. *Int. J. Numer. Methods Eng.*, 37:229–256, 1994.
- [29] Y. Vidal, P. Villon, and A. Huerta. Locking in the incompressible limit: pseudo-divergence-free element free Galerkin. *Commun. Num. Methods Eng.*, 19:725–735, 2003.
- [30] A. Ortiz, M. A. Puso, and N. Sukumar. Maximum-entropy meshfree method for compressible and near-incompressible elasticity. *Comput. Methods Appl. Mech.*, 199:1859–1871, 2010.
- [31] J. Dolbow and T. Belytschko. Volumetric locking in the element free Galerkin method. *Int. J. Numer. Methods Eng.*, 46:925–942, 1999.
- [32] M. Preisig. Locking-free numerical methods for nearly incompressible elasticity and incompressible flow on moving domains. *Comput. Methods Appl. Mech. Engrg.*, 213:255–265, 2012.
- [33] F. Auricchio, L. da Veiga Beirao, A. Buffam, C. Lovadina, and A. Reali. A fully locking-free isogeometric approach for plane linear elasticity problems: a stream function formulation. *Comput. Methods Appl. Mech. Engrg.*, 197:160–172, 2007.
- [34] T.J.R. Hughes, J.A. Cottrell, and Y. Bazilevs. Isogeometric analysis: CAD, finite elements, NURBS, exact geometry, and mesh refinement. *Comput. Methods Appl. Mech. Engrg.*, 194:4135–4195, 2005.
- [35] D. N. Arnold, R. S. Falk, and R. Winther. Finite element exterior calculus: from Hodge theory to numerical stability. *Bul. Am. Math. Soc.*, 47:281–354, 2010.
- [36] M. G. Eastwood. A complex from linear elasticity. pages 23–29. *Rend. Circ. Mat. Palermo, Serie II, Suppl.* 63, 2000.
- [37] P. G. Ciarlet and P. Ciarlet. Direct computation of stresses in planar linearized elasticity. *Math. Mod. Meth. App. Sci.*, 19:1043–1064, 2009.
- [38] I. Bijelonja, I. Demirdzic, and S. Muzaferija. A finite volume method for incompressible linear elasticity. *Comput. Methods Appl. Mech. Engrg.*, 195:6378–6390, 2006.
- [39] P. Gross and P. R. Kotiuga. *Electromagnetic Theory and Computation: A Topological Approach*. Cambridge University Press, Cambridge, 2004.
- [40] A. N. Hirani, K. B. Nakshatrala, and J. H. Chaudhry. Numerical method for Darcy flow derived using Discrete Exterior Calculus. *E-print arXiv:0810.3434v3*, 2008.
- [41] D. Pavlov, P. Mullen, Y. Tong, E. Kanso, J. E. Marsden, and M. Desbrun. Structure-preserving discretization of incompressible fluids. *Physica D*, 240:443–458, 2011.
- [42] I. Chao, U. Pinkall, P. Sanan, and P. Schröder. A simple geometric model for elastic deformations. *ACM Trans. on Graph.*, 29:38:1–38:6, 2010.
- [43] E. Kanso, M. Arroyo, Y. Tong, A. Yavari, J. E. Marsden, and M. Desbrun. On the geometric character of force in continuum mechanics. *ZAMP*, 58:843–856, 2007.
- [44] A. Yavari. On geometric discretization of elasticity. *J. Math. Phys.*, 49:022901, 2008.
- [45] J. E. Marsden and T. Hughes. *Mathematical Foundations of Elasticity*. Dover Publications, New York, 1994.
- [46] A. Yavari, J. E. Marsden, and M. Ortiz. On the spatial and material covariant balance laws in elasticity. *J. Math. Phys.*, 47:85–112, 2006.

- [47] A. Yavari and A. Goriely. Riemann-Cartan geometry of nonlinear dislocation mechanics. *Arch. Rat. Mech. Anal.*, 205:59–118, 2012.
- [48] A. Yavari and A. Goriely. Riemann-Cartan geometry of nonlinear disclination mechanics. *Math. Mech. Solids*, 18:91–102, 2013.
- [49] A. Yavari and A. Goriely. Weyl geometry and the nonlinear mechanics of distributed point defects. *Proceedings of the Royal Society A*, 468:3902–3922, 2012.
- [50] D. G. Ebin and J. E. Marsden. Groups of diffeomorphisms and the motion of an incompressible fluid. *Ann. of Math.*, 92:102–163, 1970.
- [51] R. W. Ogden. *Non-linear Elastic Deformations*. Dover Publications, New York, 1997.
- [52] M. do Carmo. *Riemannian Geometry*. Birkhäuser, Boston, 1992.
- [53] R. Abraham, J. E. Marsden, and T. Ratiu. *Manifolds, Tensor Analysis, and Applications*. Springer-Verlag, New York, 1988.
- [54] A. Yavari and A. Ozakin. Covariance in linearized elasticity. *J. Appl. Math. Phys. (ZAMP)*, 59:1081–1110, 2008.
- [55] J. E. Marsden and J. Scheurle. The reduced Euler-Lagrange equations. *Fields Inst. Comm.*, 1:139–164, 1993.
- [56] A. N. Hirani. *Discrete Exterior Calculus*. PhD thesis, California Institute of Technology, 2003.
- [57] R. R. Hiemstra, R. H. M. Huijsmans, and M. I. Gerritsma. High order gradient, curl and divergence conforming spaces, with an application to compatible NURBS-based Isogeometric Analysis. *E-print arXiv:1209.1793*, 2012.
- [58] J. Munkres. *Elements of Algebraic Topology*. Springer, New York/Addison-Wesley, Menlo Park CA, 1984.
- [59] J. Munkres. *Elementary Differential Topology*. Annals of Mathematics Studies 54, Princeton University Press, 1966.
- [60] A. N. Hirani, K. Kalyanaraman, and E. B. VanderZee. Delaunay Hodge star. *Computer-Aided Design*, 45:540–544, 2013.
- [61] E. VanderZee, A. N. Hirani, D. Guoy, and E. A. Ramos. Well-centered triangulation. *SIAM J. Sci. Comput.*, 31:4497–4523, 2010.
- [62] J. M. Lee. *Introduction to Topological Manifolds*. Springer-Verlog, New York, 2011.
- [63] P. Alfeld. Upper and lower bounds on the dimension of multivariate spline spaces. *SIAM J. Numer. Anal.*, 33:571–588, 1996.
- [64] M. E. Rudin. An unshellable triangulation of a tetrahedron. *Bull. Amer. Math. Soc.*, 64:90–91, 1958.
- [65] S. P. Timoshenko and J. N. Goodier. *Theory of Elasticity*. McGraw-Hill, New York, 1970.